Foamy Oil Flow in Porous Media

D.D. JOSEPH[1], A.M. KAMP[2], R. BAI[1], M. HUERTA[2]

[1] Univ. of Minnesota, Dept. of Aerospace Engng. & Mech, 107 Akerman Hall
110 Union Street. S.E., Minneapolis, MN 55455, USA
[2] PDVSA Intevep, PO Box 76343, Caracas 1070-A, Venezuela

September 1999
Older Version

Abstract

Certain heavy oils which foam under severe depressurization give rise to increased production and an increased rate of production under solution gas drive. The phenomenon seems to be related to the chemistry of these oils which not only stabilize foam but also stabilize dispersion of gas bubbles at lower volume ratios. We present here a mathematical model of this phenomenon which depends only on the velocity through D'Arcy's law, the pressure and the dispersed gas fraction. The theory governs only in situations in which the bubbles do not coalesce to produce the percolation of free gas. In this theory the bubbles move with the oil as they evolve. The main empirical content of the theory enters through the derivation of solubility isotherms which can be obtained from PVT data; modeling of nucleation, coalescence, bubble drag laws and transfer functions are avoided. The resulting theory is hyperbolic and nonlinear. The nonlinear equations for steady flow through a sandpack are solved by quadrature and give rise to good agreements between theory and the experiments of Maini & Sarma [1994] without fitting constants.

1 Introduction

In this paper a model is presented that is motivated by the need to explain anomalous features associated with production from reservoirs of so-called foamy oils. These oils are described by some of their properties of response to pressure declines; it is noted that they nucleate dispersed gas bubbles and display obvious foaminess in well head samples produced by solution gas drive in which oil and gas are produced by the drawdown of pressure (Huerta *et al.* [1996], Mirabal *et al.* [1996]).

When compared with the response of conventional oils, the response of foamy oils to drawdown of pressure is more favorable; primary recovery factor (percentage of the oil in the reservoir which can be recovered), the rate of production, the

volume ratio of oil to gas which is recovered and the length of time that a given pressure gradient or rate of production can be maintained are all increased substantially; the reasons for the favorable response of foamy oils in solution gas drive are not well understood and tentative explanations which have been put forward are controversial (see Maini [1996], Pooladi-Darvish and Firoozabadi [1997] and Sheng *et al.* [1999a] for recent reviews).

Foamy oils carry considerable amounts of dissolved gases in the condensed state. The relevant thermodynamic property for this is "gas solubility"; a function of temperature and pressure at equilibrium which gives the volume ratio of dispersed gas from the crude oil by outgassing. Tables of solubility of methane, carbon dioxide and other gases in various Canadian crude oils have been given by Svrcek & Mehrotra [1982], Peng *et al*. [1991] and others. The oils considered to be foamy evidently cavitate small dispersed bubbles which, under some conditions, are believed to move with the crude oil in which they are dispersed. Experiments done by Pooladi-Darvish & Firoozabadi [1997] have shown that bubbles which arise from depressurization of silicone oil and heavy crude of equivalent viscosity are very different; the bubbles in the silicone oil are larger and much more mobile than the ones in crude oil. Viscosity alone is not enough to demobilize dispersed gas; it is necessary to look at other properties like surface tension and surface active agents. Possibly there are surface active agents which are present naturally in foamy crudes which allow them to foam, but the precise agents, their composition and the mechanics by which they are released apparently have not been studied.

A "foamy oil" is a heavy oil which foams under rapid depressurization. Maini [1996] notes that "... The term "foamy oil" is often used to describe certain oils produced by solution gas drive which display obvious foaminess in wellhead samples. The primary production of heavy oil from several reservoirs in western Canada is in the form of an oil continuous foam. This foam resembles a chocolate mousse in appearance and often persists in open vessels for several hours ... " Foaming at a well head is a kind of foam formation analogous to the head on beer. To get such a head the pressure decline must be sufficiently severe to allow the bubbles which rise from outgassing of condensed gas in the bulk to accumulate at the free surface faster than they collapse. Perhaps there are surfactants in foamy oil which stabilize the films between the bubbles preventing collapse, promoting the buildup of the head. Foam stability measurements in the laboratory have shown that the foaminess of crude heavy oils is comparable to aqueous foams used for steam flooding applications (Sheng *et al*. [1996]). The outgassing of condensed gas will not lead to foam at the well head if the rate of depressurization is too low.

To create foam in a reservoir or in a sandpack it is necessary to depressurize rapidly enough to produce close packed solution gas bubbles which can undergo a topological phase change to stable films and plateau borders. This kind of "in

situ" foaming of sandpacks has been achieved in the experiments of Maini and Sarma [1994]. Gas and liquid move in lock step in these foams and lead to very high primary recovery factors. At the actual reservoir, gas fractions can be as low as 5 to 10% in oils which cannot foam but are well-dispersed and protected against coalescence, possibly by the same natural surfactants that might stabilize the foams.

In solution gas drive of foamy oil the depressurization of the sample leads to cavitation of small dispersed bubbles. The volume ratio of dispersed gas increases the volume of our composite fluid and it acts as a pump, gas coming out of solution pumps the fluid outward. This pumping action is well described by the continuity equation (4.4) which implies that in a closed volume v with boundary ∂v containing dispersed bubbles of volume fraction ϕ

$$\int_v \frac{1}{1-\phi}\frac{d\phi}{dt}dv = \oint_{\partial v} \mathbf{u}.\mathbf{n} \tag{1.1}$$

where $\mathbf{n}$ is the outward normal on ∂v and $\mathbf{u}$ is the velocity of our composite fluid.

The relative velocity of dispersed gas is important; if the bubbles coalesce and move relative to the oil more gas and less oil will be produced. Good recovery is sometimes described by a critical gas saturation value; this is the volume fraction of gas at which the gas becomes connected and starts to move. Maini [1996] identifies this critical saturation as a percolation limit, whilst Firoozabadi, Ottensen and Mikkelsen [1992] and Pooladi-Darvish and Firoozabadi [1997] identify this even by visual observation of bubbles in a viewing window. The values given by Firoozabadi *et al.* are about 5 times smaller than those given by Maini and his coworkers.

When the gas percolates, the good news about recovery is over; it is no wonder that all authors find that the critical saturation values are about the same as the primary recovery factors (which is the fraction of oil recovered by solution gas to oil in the reservoir) even when they disagree about definitions.

A few models of foamy oil flow have been put forward; each emphasize some special feature. One of the most recent models by Sheng *et al.* [1996], Sheng *et al.* [1999a] is a multiphase theory based on conservation laws with transfer from solution gas to evolved gas and from evolved gas to dispersed gas and free gas. Their theory does not seem to follow the curve of experimental values. They say that ". . . Published models include the psuedo-bubble point model (Kraus *et al.* [1993]), the modified fractional flow model (Lebel [1994]) and the reduced oil viscosity model (Claridge & Prats [1995]). Maini [1996] gave a detailed review and discussion of some of these models. These models have been used to history match heavy oil

production, but their common weakness is that the dynamic processes which are important features of foamy oil flow were not included properly. Although it may be possible to get an acceptable history match using these models, the predictive ability is likely to be limited. . . "

A more successful approach to modeling was recently advanced by Sheng *et al.* [1999b]. This model also requires the modeling of nucleation, bubble growth and disengagement of gas bubbles from the oil. The model ultimately leaves undetermined two adjustable parameters which fit the theory to experimental data better than previous models.

The present theory could be called a continuum mixture theory which is appropriate for foamy oil flow with dispersed gas of low mobility relative to the liquid and leads to three coupled nonlinear partial differential equations for $\mathbf{u}$, p and the gas fraction ϕ, five scalar equations in five unknowns. Our model has a few features in common with the excellent early work of Leibenson [1941] on the motion of gas saturated fluid in a porous media.

The model proposed here does not require information about nucleation, bubble growth, compressibility or forces which produce relative velocity. We put up a one-phase or mixture theory in which the dispersed gas is described by a gas fraction field in a single fluid in which the viscosity, density and mobility in D'Arcy's law all depend on the gas fraction. This fluid satisfies the usual D'Arcy law, and the continuity equation together with a kinetic (constitutive) equation required by the condensation and outgassing of methane (or other gases) in heavy crude. The theory depends only on parameters which can be measured in a PVT cell and sandpack. The virtue of the model is simplicity, but it can work only for relatively immobile dispersed gas bubbles in which divergence-free velocities are excluded (see the discussion following (4.4)). Certainly such a theory could not be expected to give rise to a percolation threshold or even to a critical gas fraction. We shall show that it can describe many features of solution gas drive of foamy oils in the regimes when the bubbles in the mixture are dispersed and even when they are trapped in foam.

It is our idea that the increased recovery and production are generated by the pumping of nucleating and growing gas bubbles embodied in (1.1). However recovery factors and production rates are not the same and we might test some ideas: if two foamy oils have the same viscosity, the one with higher solubility will have higher primary recovery and production rate; if two foamy oils have the same solubility, the one with lower viscosity will have a higher rate of production but a lower primary recovery. If the oil foams in situ, oil and gas move in lock step and the primary recovery factor increases while due to the increased viscosity of foam the rate of production decreases.

2 Solubility Isotherms

In the experiments of Svrcek & Mehrotra [1982] the pressure is dropped from p and T to p_{ref} and T_{ref} where in the experiments p_{ref} is atmospheric and $T_{\text{ref}} = 373.2°\text{K}$. It is assumed that all the gas in the live oil at p, T comes out. Defining now:

$V_g(p,T)$ is the volume of dispersed gas,
$V_l(p,T)$ is the volume of live oil,
$V^*(p,T)$ is the volume of dispersed gas which vaporizes from the condensed gas when p, T are dropped to $p_{\text{ref}}, T_{\text{ref}}$.

In this model we avoid all constitutive equations regarding nucleation rates and bubble growth. In our model we have only a mixture of liquid and dispersed gas, and the dispersed gas enters only through the volume fraction

$$\phi = \frac{V_g}{V_l + V_g}. \tag{2.1}$$

Equation (2.1) may be solved for

$$V_g = \frac{\phi V_l}{1 - \phi}. \tag{2.2}$$

Svrcek and Mehrotra [1982] give volumetric solubility curves (CO_2 and methane in figure 2.1). In these figures

$$\hat{V} = V^*/V_l(p,T) \tag{2.3}$$

is the ratio between the volume of gas that can be evolved out of bitumen when the pressure is dropped to less than one atmosphere at a temperature of 100 °C and the original volume of bitumen. We can assume that this tells you how much dispersed gas can come out of solution of condensed gas which is at a saturation value at any pressure and temperature. We are going to assume that this $\hat{V}$ determines the dispersed gas fraction ϕ following an argument put forward in what is to follow.

In the present approach we have no way to predict the size distribution of gas bubbles. This means that we are free to choose the size and distribution to measure $\hat{V}$ and the most convenient choice is when all the released gas is collected at the top of a PVT such as in the experiment of Svrcek & Mehrotra. Figure 2.2 describes such a depressurization experiment.

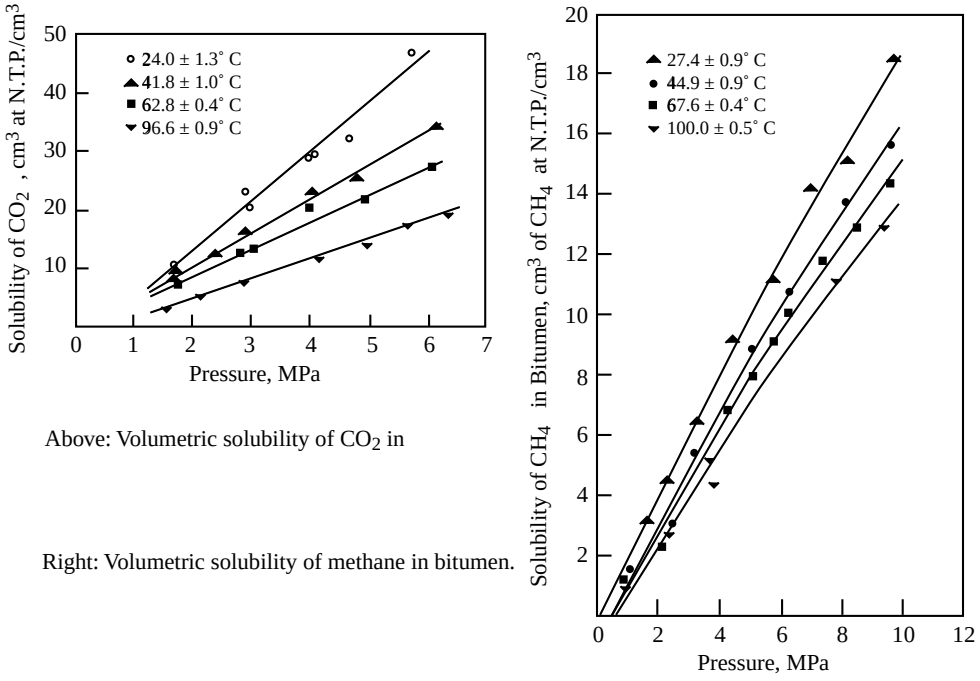

Above: Volumetric solubility of CO_2 in

Right: Volumetric solubility of methane in bitumen.

Figure 2.1: Solubility curves: $\hat{V}$ vs. p (Svrcek and Mehrotra [1982]).

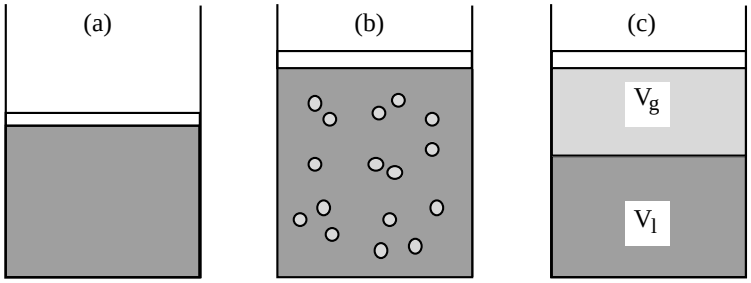

Figure 2.2: Depressurization experiment in PVT cell at constant temperature; the oil is indicated in dark gray, the gas in light gray. (a) Dissolved gas at pressure p and temperature T. (b) Just after the pressurization, pressure p_{ref} and temperature T_{ref}. (c) Finally all the gas percolates out and $\hat{V} = V^*/V_l$ can be measured.

Their data show that

$$p - p_{\text{ref}} = \hat{\gamma}(T)\hat{V} \tag{2.4}$$

where $\hat{\gamma} = dp/d\hat{V}$ is the slope of the solubility isotherms shown in figure 2.1. This slope is approximately constant. Here we have chosen p_{ref} as a small pressure at which a negligible amount of gas is dissolved in the oil. For practical purposes this could be standard (atmospheric) pressure.

2.1 Solubility Isotherms I

We first suppose that all the gas which comes out of solution is dispersed and does not percolate or foam. In the experiments in figure 2.1, we must suppose that the nucleation, growth and compressibility of gas bubbles are working, but these microstructural features are not monitored in these experiments which give only the solubility $\hat{V}$. This is also what we do in the mathematical model.

To convert (2.4) into a relation between p and ϕ at equilibrium we note that the total mass M of gas in the live oil is invariant, independent of p and T and

$$M = M_g(p,T) + M_c(p,T) \tag{2.5}$$

where

$M_g(p,T)$ is the mass of dispersed gas.
$M_c(p,T)$ is the mass of condensed gas.

Since the mass of condensed gas does not change when it is vaporized and assuming that this vapor is a perfect gas, we have

$$M_c = p_{\text{ref}} V^* / R T_{\text{ref}} \tag{2.6}$$

where R is the gas constant. From the same gas law

$$M_g = p V_g / R T. \tag{2.7}$$

Hence, from (2.5), (2.6) and (2.7) we have

$$M = \frac{p V_g}{RT} + \frac{p_{\text{ref}} V^*}{R T_{\text{ref}}} \tag{2.8}$$

and, using (2.3) and (2.4)

$$M = \frac{p V_g}{RT} + \frac{p_{\text{ref}}}{R T_{\text{ref}}} \left(\frac{p - p_{\text{ref}}}{\hat{\gamma}} \right) V_l. \tag{2.9}$$

We next introduce the bubble point pressure $\tilde{p}$ as the pressure at which there is no dispersed gas, all the gas is condensed in the live oil so that $V_g = 0; \tilde{V} \stackrel{\text{def}}{=} \hat{V}$ when $V_g = 0$ and from (2.4)

$$\tilde{p} - p_{\text{ref}} = \hat{\gamma}(T) \tilde{V} \tag{2.10}$$

where

$$\tilde{V}(\tilde{p}, T) = V^*(\tilde{p}, T) / V_l(\tilde{p}, T) \tag{2.11}$$

as in the cartoon of figure 2.3.

Since M is invariant, we may evaluate (2.8) at the bubble point

$$M = \frac{p_{\text{ref}}}{R T_{\text{ref}}} V_l(\tilde{p}, T) \tilde{V}(\tilde{p}, T). \tag{2.12}$$

Using (2.10) to eliminate $\tilde{V}$ in (2.12) and equating (2.12) and (2.9) we get

$$\frac{T_{\text{ref}}}{T} \frac{p}{p_{\text{ref}}} V_g + \left(\frac{p - p_{\text{ref}}}{\hat{\gamma}} \right) V_l(p, T) = \left(\frac{\tilde{p} - p_{\text{ref}}}{\hat{\gamma}} \right) V_l(\tilde{p}, T) \tag{2.13}$$

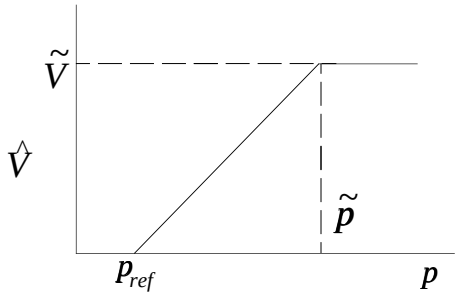

Figure 2.3: Solubility isotherm used in this model.

In most depressurization experiments the change of liquid volume due to outgassing and compressibility is small and $V_l(p,T) \approx V_l(\tilde{p},T)$. In this case the terms proportional to p_{ref} in (2.13) subtract out and after replacing V_g with $\phi V_l/(1-\phi)$ we get

$$\beta\frac{\phi}{1-\phi} = \frac{\tilde{p}-p}{p} \tag{2.14}$$

where

$$\beta = \frac{T_{\text{ref}}}{T}\frac{\hat{\gamma}}{p_{\text{ref}}} \tag{2.15}$$

is completely determined by the solubility isotherm in figure 2.1. Since the variation of T is small on an absolute scale, the values T/T_{ref} for the isotherms in figure 2.1 are just slightly larger than one.

The variable $\hat{V}$ is called *gas-oil ratio* and $\tilde{V}$ is the gas-oil ratio at saturation pressure. From (2.10):

$$\hat{\gamma}(T) = \frac{\tilde{p}-p_{\text{ref}}}{\tilde{V}}. \tag{2.16}$$

Substituting this value of $\hat{\gamma}$ in (2.15)

$$\beta = \frac{T_{\text{ref}}}{T}\frac{\tilde{p}-p_{\text{ref}}}{p_{\text{ref}}\tilde{V}}. \tag{2.17}$$

In most practical situations $\tilde{p} \gg p_{\text{ref}}$ so that from (2.17)

Oil	β
Lloydminster	3.40
Lindbergh	3.17
Cerro Negro	3.53

Table 2.1: Solubility coefficients for some heavy oils.

$$\beta = \frac{T_{\text{ref}}}{T}\frac{\tilde{p}}{p_{\text{ref}}\tilde{V}} \tag{2.18}$$

It is customary in the oil industry to characterize live oil by its saturation pressure $\tilde{p}$ and its gas-oil ratio $\tilde{V}$ at saturation pressure. By virtue of (2.18) one can calculate the solubility parameter β. Note that in most experiments p_{ref} is chosen as atmospheric pressure and T_{ref} as 60°F = 15.6°C.

Values for β for two Canadian heavy oils, Lloydminster and Lindbergh (Maini & Sarma, 1994) and for a Venezuelan heavy oil, Cerro Negro, are given in table 2.1. Graphs of the isotherm (2.14) for various values of β are shown in figure 2.5.

It can be noted that the solubility value for heavy crude oils from very different regions are very close, which indicated that they contain similar amounts of dissolved gases.

When ϕ and p satisfying (2.14) vary from point to point

$$\nabla p = \frac{-\beta p^2}{\tilde{p}(1-\phi)^2}\nabla\phi. \tag{2.19}$$

According to D'Arcy's law, $\mathbf{u} = -\lambda\nabla p$ where λ is the mobility of the foamy mixture in the porous media; hence the fluid flows up the bubble gradient toward regions in which there are more bubbles where the pressure is smaller.

Departures from the equilibrium solubility relation (2.14) are indicated as *supersaturation* or *subsaturation.* Defining the function

$$f(p,\phi) \stackrel{\text{def}}{=} \tilde{p} - p - \beta p\phi/(1-\phi) \tag{2.20}$$

supersaturation $(f > 0)$ corresponds to having more gas dissolved than there should be under thermodynamic equilibrium; subsaturation $(f < 0)$ corresponds to having less gas dissolved than there should be under equilibrium. Supersaturation occurs when the pressure in the reservoir is drawn down, but the oil cannot evolve

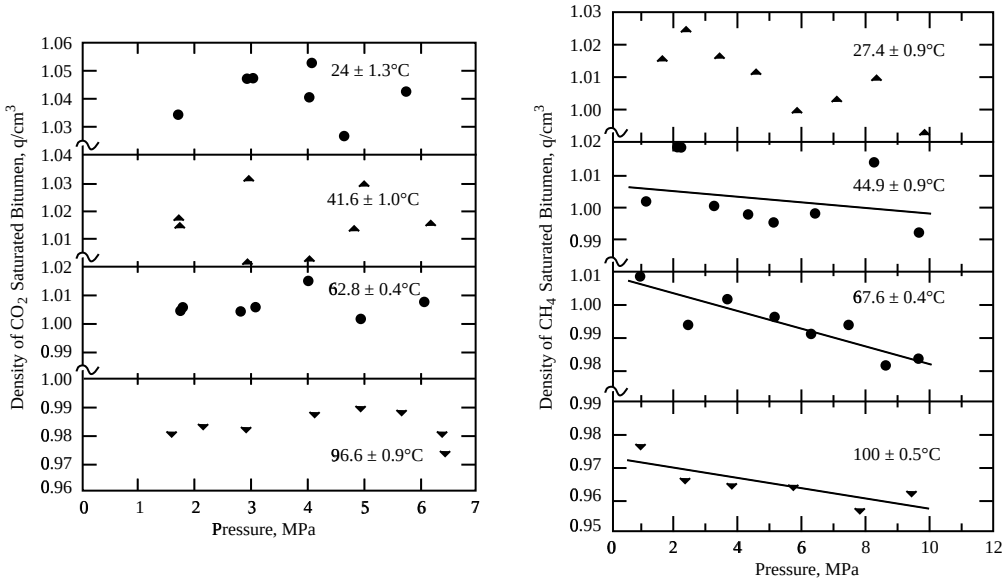

Figure 2.4: The density of bitumen and condensed gas mixtures. The density is nearly constant over very wide ranges of pressure. We can imagine that the mixture density is independent of pressure. Since gas solubility is a strong function of pressure; the density is also more or less independent of the fraction of dissolved gas at constant temperature (Svrcek & Mehrotra [1982]).

gas fast enough to keep up with the depressurization. Subsaturation, on the other hand, occurs when there is not enough gas available to dissolve in order to satisfy thermodynamic equilibrium at prevailing reservoir pressure and temperature. The function f in our theory is thus an indicator for departure from equilibrium solubility.

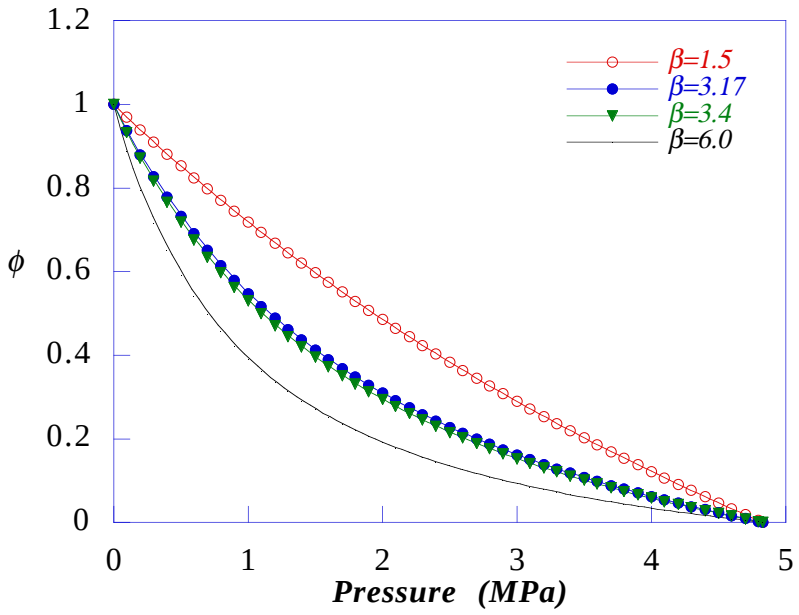

Figure 2.5: Graphs of the solubility isotherm (2.14) for various values of β. The limits of validity of the dispersed gas model can be roughly set at a close packing value, say $\phi_c = 0.68$. When $\phi > \phi_c$ some bubbles must touch and form foam film or to coalesce. This implies that results for drawdown greater than those for which $\phi = 0.68$ must take into account foaming and fingering of free gas.

2.2 Solubility Isotherms II

Consider a drawdown to atmospheric pressure $p_a = 10^6$dynes/cm^2 from a saturation pressure $\tilde{p} = 4.83 \times 10^7$dynes/cm^2 as in the experiment of Maini & Sarma [1994]. Using β = 3.4 for Lloyminster (from table 2.1) and evaluating the gas fraction of $\phi = \phi_a$ at atmospheric pressure we find

$$\phi_a = 0.93 \tag{2.21}$$

This is too much gas to exist as a bubbly dispersion; either the bubbly mixture passed into foam near to some outical value, say

$$\phi = \phi_c = 0.680 \tag{2.22}$$

or close packing or else some of the bubbles coalesced as free gas which fingers out of the sandpack. Probably foam and free gas both evolve at the outlet of a closed sandpack after a sudden drawdown to atmospheric from high saturation.

We may acknowledge the condition of close packing associated with change of phase to foam or free gas by rethinking and rewriting the derivation of (2.14) as

$$\beta \cdot \frac{\phi}{\phi_c - \phi} = \frac{(\tilde{p} - p_c) - (p - p_c)}{p - p_c} \tag{2.23}$$

where p_c is some pressure at which the gas fraction is ϕ_c. Equation (2.23) is in the same form as (2.14) with ϕ/ϕ_c replacing ϕ and $p - p_c$ replacing p.

We also note that the physics of supersaturation is complicated by the fact that bubbles cannot nucleate continuously and that the mechanism by which they nucleate is still not well understood. A bubble which might form in crude oil by the vaporization of dissolved gas at supersaturated conditions can be expected to satisfy Laplace's law

$$p_{vapor} - p = 2\gamma/R \tag{2.24}$$

where γ is surface tension (say 30 dynes/cm) and R is the bubble radius. Under mildly supersaturated conditions p is slightly smaller than the vapor pressure p_{vapor}; hence, R satisfying (2.24) cannot be very small.

It is argued that the vaporization of dissolved gas under supercritical conditions requires the simultaneous presence of undissolved gas hidden in crevices of impurities which are wet by gas preferentially. The curvature of the gas-oil interface in such a crevice is opposite to a bubble and it is controlled by capillarity rather than interfacial tension. The supersaturated dissolved gas vaporizes at the undissolved gas hidden in the crevice and the volume of the gas grows there until a bubble breaks away restoring the nucleation site to its original condition. The train of gas bubbles which emanate usually from a single site on a glass of beer as the gas comes out of the solution is a convenient example of outgassing at a nucleation site. The pore walls in a porous media are nucleation sites for outgassing of foamy oil. The possibility that asphaltenes in the oil are nucleation sites for dissolved gas is a current but unresoloved question.

In deriving (2.14), or (2.23), we have assumed the continuity of pressure across the bubble surface, ignoring the small pressure drop implied by (2.24).

In the sequel, we will base our analysis on the solubility isotherm I, given by (2.14), understanding that the theory is expected to lose validity when the drawdown is large enough to produce close packing. It is certain that we can achieve

better agreements with experiments by using β and ϕ_c as fitting parameters, but our purpose is better served by carrying the *ab initio* theory without any wiggle room through to conclusion.

3 Live oil and dead oil

Oil without dissolved gas is called dead oil. Oil saturated with dissolved gas is called live oil. The dissolved gas can be considered condensed and live oil is a mixture of miscible liquids, dead crude oil and condensed gas. The mixture of miscible liquids is like glycerin and water with the caveat that the oil and dissolved gas do not mix in all proportions; the fraction of dissolved gas at saturation is a function of temperature and pressure. The weight fraction of dissolved gases corresponding to figure 2.1 ranges from 0.3 to 6%. (See the tables in Svrcek & Mehrotra [1982]).

The viscosity of live oil can be orders of magnitude smaller than the viscosity of dead oil; the viscosity of live oil is a strongly decreasing function of the amount of dissolved gas in solution just as the viscosity of glycerol strongly decreases with the water fraction. In a pressure decline the viscosity of the live oil will increase because less gas is dissolved and because the presence of dispersed gas should increase the viscosity of the composite fluid.

We may seek to answer the question "what is the density of the dissolved gas in solution." We are not able to measure the density of the liquid gas in oil, but the density ρ of the mixture is available in data presented by Svrcek and Mehrotra and reproduced in figure 2.4. Let us note that this data shows that the density of the CO_2 in bitumen is a strong function of the pressure; hence figure 2.4 shows that the density of the not saturated bitumen is independent of the volume ratio Ψ of soluble gas in bitumen. Dissolved methane has a density only slightly different than bitumen (see figure 2.1). A theory of miscible mixtures which applies to live oil can be found in Chapter X of Joseph & Renardy [1992].

4 Model description

In this model we avoid all constitutive equations regarding nucleation rates and bubble growth. In our model we have only foamy oil and dispersed gas and the dispersed gas enters only through its volume ratio ϕ. The model combines D'Arcy's law, with a ϕ dependent mobility, a mass conservation law for ideal mixtures together with a constitutive equation governing the evolution of departures from equilibrium solubility. For out of equilibrium events gradients and time derivatives are crucial. The time derivatives which are used here have a material derivative

$$\frac{D}{Dt} = \alpha \frac{\partial}{\partial t} + \mathbf{u} \cdot \nabla \tag{4.1}$$

where α is the porosity. The continuity equation is given by

$$\frac{d\rho}{d\phi}\frac{D\phi}{Dt} + \rho(\phi)\text{div } \mathbf{u} = 0 \tag{4.2}$$

where

$$\rho(\phi) = \rho_g \phi + \rho_l(1-\phi) \approx \rho_l(1-\phi) \tag{4.3}$$

because $\rho_g \ll \rho_l$ where ρ_l is the density of live oil which depends only weakly on the volume ratio of dissolved gas. Combining (4.3) and (4.2) we find that

$$\frac{D\log(1-\phi)}{Dt} + \text{div } \mathbf{u} = 0 \tag{4.4}$$

Equation (4.4) restricts the theory to dispersions of low mobility relative to the suspending liquid. In any motion $\mathbf{u}(\mathbf{x}, t)$ of the composite which is divergence free div$\mathbf{u} = 0$, the dispersed gas fraction satisfies

$$\frac{D\phi}{Dt} = 0.$$

This implies that the volume ratio does not change on material particles of the composite fluid on divergence free motions.

Bubbles rising under gravity would lead to divergence free motions as would any motion of the bubbly mixture in which dispersed bubbles do not nucleate, diffuse or compress. Motions with non-zero divergence satisfy (1.1); the flux out of any closed volume, over which the div $\mathbf{u}$ does not sum to zero, must be non zero. This is the simplified way that our theory accounts for nucleation and diffusion.

Turning next to D'Arcy's law we let x increase in the direction of gravity. Then

$$\mathbf{u} = -\lambda\{\nabla p - \rho g \mathbf{e}_x\} \approx -\lambda\{\nabla p - \rho_l(1-\phi)\mathbf{e}_x\} \tag{4.5}$$

where

$$\lambda(\phi) = \kappa(\phi)/\mu(\phi) \tag{4.6}$$

is the mobility, $\mu(\phi)$ is the viscosity of live oil with dispersed gas of volume ratio ϕ and $\kappa(\phi)$ is the permeability.

4.1 Constitutive equations relating the dispersed gas fraction to the pressure

We are proposing models in which the basic variables are the pressure and dispersed gas fraction and are such that disturbed systems which are not forced will relax to equilibrium with pressure and temperature on the solubility isotherm $f(p,\phi) = 0$ given by (2.4). There are many possible ways to build models with the above properties. The simplest conceptual model with the desired properties is a first evolution model

$$\tau \frac{Df}{Dt} = -f \tag{4.7}$$

which guarantees that a disturbed stationary system will relax exponentially

$$f(p,\phi) = f(p,\phi_o) exp\left(-\frac{t}{\alpha\tau}\right)$$

Though (4.7) is conceptually simple, it is a mathematically difficult and strongly nonlinear problem when there is flow. This problem will be studied in a future work.

The most general *linear* evolution equation is assumed in the form

$$\tau \frac{Dp}{Dt} + \gamma\tau \frac{D\phi}{Dt} = f(p,\phi)$$

where $f(p,\phi)$ is given by (2.4) and τ and γ are to-be-determined constants. The determination of optimum values for γ and τ is a complicated problem which must involve mathematical analysis and comparisons of predictions with experiment. Here we take only some preliminary steps toward the solution of this problem.

4.2 Hyperbolic theory

In the work which follows we put $\gamma = 0$. The equation

$$\tau \frac{Dp}{Dt} = f(p,\phi) \tag{4.8}$$

is a Maxwell-like relaxation theory and τ is a relaxation time.

We shall show that the Maxwell type equation (4.8) leads to a hyperbolic system in which pressure changes propagate by waves. On the other hand, the equation in which the pressure derivative is neglected so that $\gamma\tau\frac{D\phi}{Dt} = f(p,\phi)$ leads to

parabolic propagation. The propagation of fronts of nucleating bubbles associated with the hyperbolic theory (4.8) is appealing and is our focus in this paper.

Collecting our equations, we have

$$\left.\begin{aligned} \tau\left(\alpha\frac{\partial p}{\partial t}+\mathbf{u}\cdot\nabla p\right) &= f(p,\phi) \\ &= \tilde{p}-p-\beta p\phi/(1-\phi)\,, \\ \frac{1}{1-\phi}\left(\alpha\frac{\partial \phi}{\partial t}+\mathbf{u}\cdot\nabla\phi\right) &= \operatorname{div}\mathbf{u}\,, \\ \mathbf{u} &= -\lambda\nabla p+\lambda\rho_l g(1-\phi)\mathbf{e}_x \end{aligned}\right\} \tag{4.9}$$

The parameters defining (4.9) are material parameters associated with solubility β in the function $f(p,\phi)$, porous material parameter α, mobility $\lambda(\phi)$, which is the ratio of permeability upon the viscosity of the foamy mixture, and the relaxation time τ. The relaxation time is a new parameter introduced here and it may be determined by wave speed measurements (see section 5).

The velocity $\mathbf{u}$ may be eliminated from (4.9). Thus,

$$\left.\begin{aligned} &\tau\left\{\alpha\frac{\partial p}{\partial t}-\lambda|\nabla p|^2+\lambda\rho_l g(1-\phi)\frac{\partial p}{\partial x}\right\}=\tilde{p}-p-\frac{\beta p\phi}{(1-\phi)}, \\ &\frac{1}{1-\phi}\left\{\alpha\frac{\partial\phi}{\partial t}-\lambda\nabla p\cdot\nabla\phi\right\}= \\ &\qquad -\operatorname{div}(\lambda\nabla p)-2\lambda\rho_l g\frac{\partial\phi}{\partial x}+\lambda'\rho_l g(1-\phi)\frac{\partial\phi}{\partial x} \end{aligned}\right\} \tag{4.10}$$

The system (4.10) is second order and should be solvable for two-end conditions. These conditions may be expressed in terms of p or ϕ or a combination of these. However, though it is clear that the pressure and superficial velocity ought to be continuous in the whole domain and at its boundaries, the continuity of ϕ is not required. We control and prescribe the pressure, or velocity. Suppose that we put the gravity terms in (4.10) to zero; then (4.10) $_1$ may be solved for ϕ and after substituion of the result in (4.10) $_2$ this becomes an equation in p alone. We solve the p equation; then (4.10) $_1$ gives ϕ in terms of p.

The system (4.9) may be regarded as describing the flow of a relaxing compressible fluid through a porous media. To see this, we replace ϕ with $\rho = \rho_l(1-\phi)$, using (4.3). Then (4.9) may be written as

$$\left.\begin{array}{c} \tau(\alpha\frac{\partial p}{\partial t} + \mathbf{u}\cdot\nabla p) = \tilde{p} - p - \beta p\frac{\rho_l - \rho}{\rho}, \\ \alpha\frac{\partial \rho}{\partial t} + \mathbf{u}\cdot\nabla\rho + \rho\,\mathrm{div}\,\mathbf{u} = 0, \\ \mathbf{u} = -\lambda\nabla p + \lambda g\rho\mathbf{e}_x \end{array}\right\} \tag{4.11}$$

5 Constant state solutions

5.1 Constant state solutions and drainage

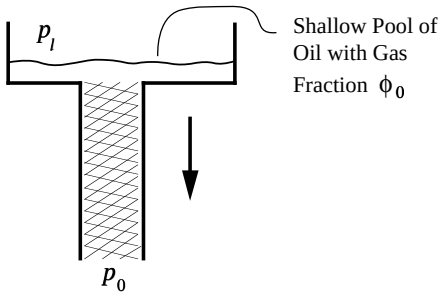

Figure 5.1: Sandpack enclosed in a pressure vessel set at pressure p_0. The supply of oil with dispersed gas fraction ϕ_0 keeps the small head at very small height. The oil and gas bubbles drain at a measured velocity u_0; then $\lambda(\phi_0) = \frac{u_0}{\rho_l g(1-\phi_0)}$

The constant state solution are uniform solutions p_0, $\phi_0, \mathbf{u}_0$ of (4.9), p_0 and ϕ_0 satisfying

$$f(p_0, \phi_0) = \tilde{p} - p_0 - \beta p_0\phi_0/(1-\phi_0) = 0 \tag{5.1}$$

and

$$\mathbf{u}_0 = \mathbf{e}_x u_0, \quad u_0 = \lambda(\phi_0)\rho_l g(1-\phi_0) \tag{5.2}$$

The constant state solution is a drainage flow; this flow may be used to determine the mobility $\lambda(\phi)$ (figure 5.1)

5.2 Perturbations of the constant state; wave speeds

If the perturbations $p', \phi', \mathbf{u}'$ of $p_0, \phi_0, \mathbf{u}_0$ are small, then

$$\tau\left(\alpha\frac{\partial p'}{\partial t} + u_0\frac{\partial p'}{\partial x}\right) + ap' + b\phi' = 0 \tag{5.3}$$

where

$$a = 1 + \frac{\beta\phi_0}{1-\phi_0}, b = \frac{\beta p_0}{(1-\phi_0)^2}$$

$$\frac{1}{1-\phi_0}\left(\alpha\frac{\partial \phi'}{\partial t} + u_0\frac{\partial \phi'}{\partial x}\right) - \text{div}\,\mathbf{u}' = 0 \tag{5.4}$$

$$\mathbf{u}' = -\lambda_0\nabla p' - \lambda'\rho_l(1-\phi_0)g\phi'\mathbf{e}_x + \frac{\lambda_0\rho_l g\mathbf{e}_x\phi'}{2} \tag{5.5}$$

When gravity is unimportant, as in a vertical sandpack, these equations reduce to

$$\tau\alpha\frac{\partial p'}{\partial t} + ap' + b\phi' = 0 \tag{5.6}$$

$$\alpha\frac{\partial \phi'}{\partial t} + (1-\phi_0)\lambda_0\nabla^2 p' = 0 \tag{5.7}$$

We may eliminate p' or ϕ' from (5.6) or (5.7); in both cases we find the telegraph equation

$$\frac{\partial^2 p'}{\partial t^2} + \frac{a}{\tau\alpha}\frac{\partial p'}{\partial t} = c^2\nabla^2 p' \tag{5.8}$$

where

$$c = \left\{\frac{b(1-\phi_0)\lambda_0}{\tau\alpha^2}\right\}^{\frac{1}{2}}$$

is a wave speed. The waves are damped by the first derivative term in (5.8). If the relaxation time tends to zero then wave propagation gives way to diffusion

$$\frac{\partial p'}{\partial t} = \frac{(1-\phi_0)\lambda_0 b}{\alpha a}\nabla^2 p' \tag{5.9}$$

6 Sandpack experiments

Sandpack experiments are used as laboratory surrogates for the flow of oil and gas in porous reservoirs. In figure 6.1 a cartoon of a typical sandpack experiment copied from a paper by Sheng *et al.* [1996] is displayed. The pack may be loaded with sand from reservoirs.

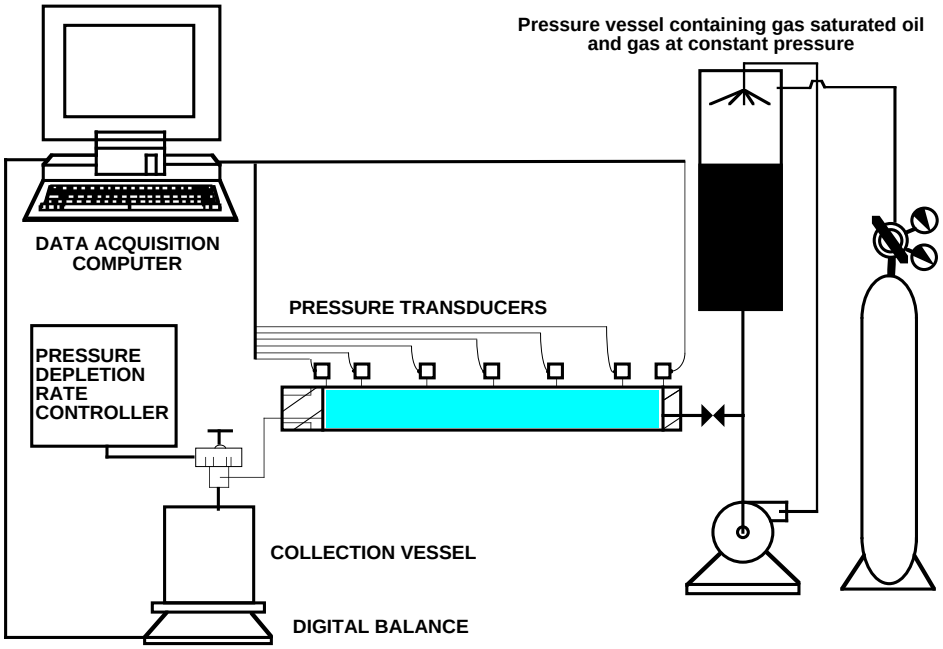

Figure 6.1: Cartoon of a sandpack experiment. Live oil can be injected at the inlet and a pressure depletion rate controller is at the outlet. Different experiments are described by prescribed conditions at the inlet and outlet.

Sandpacks provide an excellent way to get precise data under controlled conditions simulating flow in reservoirs; they are convenient for mathematical modeling because they lend themselves to one dimensional treatments. It is useful to look at these one-dimensional models for horizontal sandpacks in which gravity may be neglected and for vertical flow in which gravity may be important. In both these cases we have our governing equation (4.10) with $\nabla = e_x \partial / \partial x$. Terms proportional to gravity are put to zero in horizontal sandpacks.

Different experiments can be carried out in a sandpack corresponding to different conditions listed below.

Closed inlet. ($x = L$) $u(L,t) = 0$ hence, from (4.9) $_3$, we have

$$\frac{\partial p}{\partial x}(L,t) - \rho_l g\big(1 - \phi(L,t)\big) = 0 \tag{6.1}$$

A pressure gradient is generated by gravity in a vertical sandpack with a closed end at $x = L$. The liquid will be held in the pack by capillarity (which is not explicitly considered in this model) unless it is pushed out by nucleating bubbles.

Pressure drawdown at the outlet ($x = 0$)

$$p(0,t) = \tilde{p} - g(t) \tag{6.2}$$

where $g(0) = 0$ and $g(\infty) = p_\infty < \tilde{p}$. At $t = 0$ the sandpack has no dispersed bubbles and as $t \to \infty$ the pressure becomes uniform. A linear prescription of pressure depletion

$$\begin{array}{l} p = \tilde{p} - At \quad \text{for} \quad 0 \le t \le t_0 \\ p = p_\infty \quad \text{for} \quad t > t_0 \end{array} \tag{6.3}$$

is useful for comparing fast (A large) and slow depletion (A small). The fastest depletion is a step change of pressure

$$p(0,t) = \tilde{p} - (\tilde{p} - p_\infty)H(t) \tag{6.4}$$

where $H(t)$ is the Heaviside function.

Prescribed velocity at the outlet

$$u(0,t) = -\lambda(\phi)\left\{\frac{\partial p}{\partial x}(0,t) - \rho_l g(1-\phi)\right\} \tag{6.5}$$

is prescribed at $x = 0$. If we withdraw very rapidly, $u(0,t)$ is large, the pressure at the inlet will decline, rapidly nucleating gas. In the limit, all of the material will be gas $\phi = 1$; physically one might think of dry foam.

Open inlet. If the pressure at the inlet is prescribed at a value greater than the final outlet, and both pressures are constant in time, then a steady flow of live oil from the reservoir at the inlet to the outlet will be established. It is then of interest to predict and monitor the gas fraction distribution $\phi(x,t)$ during the transient and the final steady state (see section 9).

7 Pressure decline in a closed horizontal sandpack

At $t = 0$ live oil with no dispersed bubbles fills the sandpack

$$\phi(x,0) = 0, p(x,0) = \tilde{p}, u(x,0) = 0 \tag{7.1}$$

The velocity vanishes at the closed inlet. Hence

$$\frac{\partial p}{\partial x}(L,t) = 0 \tag{7.2}$$

The pressure decline at the outlet is given by

$$p = \begin{cases} \tilde{p} - At, 0 < t < t_0 \\ p_0, \qquad t > t_0 \end{cases} \tag{7.3}$$

where A represents the rate of decline.

From (4.10) we form the governing equations for $p - \tilde{p} = \pi (< 0)$.

$$\tau \left\{ \alpha \frac{\partial \pi}{\partial t} - \lambda \left(\frac{\partial \pi}{\partial x} \right)^2 \right\} = -\pi - \beta \frac{(\tilde{p} + \pi)\phi}{1 - \phi} \tag{7.4}$$

$$\alpha \frac{\partial \phi}{\partial t} - \lambda \frac{\partial \pi}{\partial x} \frac{\partial \phi}{\partial x} + (1 - \phi) \frac{\partial}{\partial x} \left(\lambda \frac{\partial \pi}{\partial x} \right) = 0 \tag{7.5}$$

Solutions of (7.1) through (7.4) will require numerical integration.

7.1 Telegraph equation

We may however hope to solve the linearized version of these equations, (5.6) and (5.7) with $\phi_0 = 0, a = 1, b = \beta\tilde{p}$. The governing telegraph equation is in the form

$$\frac{\partial^2 \pi}{\partial t^2} + \frac{1}{\tau\alpha} \frac{\partial \pi}{\partial t} = c^2 \frac{\partial^2 \pi}{\partial x^2} \tag{7.6}$$

$$c = \left\{ \frac{\beta \tilde{p} \lambda_0}{\tau \alpha^2} \right\}^{\frac{1}{2}} \tag{7.7}$$

and it can be solved relative to initial conditions at saturation

$$\pi(x,0) = 0 \tag{7.8}$$
$$\phi(x,0) = 0 \tag{7.9}$$

for $0 \leq x \leq L$, and to prescribed inlet and outlet conditions. At a closed inlet the velocity vanishes, hence

$$\frac{\partial \pi}{\partial x}(L,t) = 0. \tag{7.10}$$

At the outlet, we carry out a linear drawdown

$$\pi(0,t) = \begin{cases} -At, & 0 \leq t < t_0 \\ -At_0, & t \geq t_0 \end{cases} \tag{7.11}$$

The linearized theory is valid only for very small values of At_0. We must disallow step changes of π, however small. To see this, we note that the linearization of (7.4) around (7.8) and (7.9) gives rise to

$$\tau\alpha \frac{\partial \pi}{\partial t} = -\pi - \beta\tilde{p}\phi \tag{7.12}$$

so that ϕ is small only if $\frac{\tau\alpha}{\beta\tilde{p}}\frac{\partial \pi}{\partial t}$ is small, which cannot be true for step changes in π. Though conditions on ϕ are not required to solve the telegraphers equation system (7.6)–(7.11) for π, we find that the drawdown condition (7.11) implies that

$$\phi(0,t) = \frac{1}{\beta\tilde{p}} \begin{cases} At + \tau\alpha A, & 0 \leq t < t_0 \\ At_0, & t \geq t_0 \end{cases} \tag{7.13}$$

At $t = t_0$ there is a discontinuity of ϕ corresponding to the initiation of a stopping wave. Obviously the fraction of dispersed gas at the outlet is an increasing function of the drawdown rate A.

Turning next to the solution of (7.6)–(7.11), we change variables

$$\left.\begin{aligned} \pi &= -\alpha\tau A\theta \\ x &= c\tau\alpha\chi \\ t &= \tau\alpha T \end{aligned}\right\} \tag{7.14}$$

$$\frac{\partial^2\theta}{\partial T^2} + \frac{\partial\theta}{\partial T} = \frac{\partial^2\theta}{\partial\chi^2} \tag{7.15}$$

$$\theta(\chi, 0) = 0 \quad \text{for} \quad 0 \le \chi \le l, \tag{7.16}$$

$$\frac{\partial\theta}{\partial\chi}(l, T) = 0 \tag{7.17}$$

$$\theta = \begin{cases} T, & 0 \le T < T_0 \\ T_0, & T \ge T_0 \end{cases} \tag{7.18}$$

where

$$l = L/c\tau\alpha \quad \text{and} \quad T_0 = t_0/\tau\alpha. \tag{7.19}$$

To solve (7.15)–(7.18) we introduce our auxiliary problem for

$$\psi \stackrel{\text{def}}{=} \frac{\partial\theta}{\partial T} \tag{7.20}$$

given $\psi(\chi, T) = \partial\theta/\partial T$, we may find

$$\theta(\chi, T) = \int_0^T \psi(\chi, T')dT' \tag{7.21}$$

by integration. After differentiating (7.15–7.17) with respect to T, we find that ψ satisfies

$$\frac{\partial^2\psi}{\partial T^2} + \frac{\partial\psi}{\partial T} = \frac{\partial^2\psi}{\partial\chi^2}, \tag{7.22}$$

$$\psi(\chi, 0) \equiv 0 \quad \text{for} \quad 0 \le \chi \le l, \tag{7.23}$$

$$\frac{\partial\psi}{\partial\chi}(l, T) = 0 \tag{7.24}$$

$$\psi(0, T) = H(T) - H(T - T_0) \tag{7.25}$$

where $H(T)$ is a unit step function.

It should be understood that the solution does not rise above zero until it is struck by the wave moving with velocity c. Hence $\pi(x,t)$ is different from '0 only when $x < ct$ and $t < t*$ where $t*$ is the time of first reflection defined by

$$L = ct*$$

We will focus our attention on wave propagation to short times, $t < t*$ and $t < t_0$ where t_0 is the time at which the drawdown is stopped and we could choose this stopping time $t_0 < t*$ to be after the wave has reflected off the wall at $x = L$.

Short times mean that $T < T*$ and $T < T_0$. The functions $\theta(\chi, T)$ and $\psi(\chi, T)$ are different from zero only when $\chi < T$ and for short times we may replace (7.18) with

$$\theta(0,T) = T \tag{7.26}$$

and (7.25) with

$$\psi(0,T) = H(T)\ . \tag{7.27}$$

The solution of (7.22), (7.23), (7.24) and (7.27) can be found in Carlslaw and Jaeger [1949] in the form

$$\psi(\chi,T) = H(T-\chi) f(\chi,T) \tag{7.28}$$

where

$$f(\chi,T) = e^{-\chi/2} + \frac{\chi}{2}\int_{\chi}^{T}\left[\frac{e^{-\sigma/2}}{\sqrt{\sigma^2-\chi^2}} I_1(\frac{1}{2}\sqrt{\sigma^2-\chi^2})\right] d\sigma$$

and I_n is the Bessel function of imaginary argument such that $I_1(x) = dI_0(x)/dx$. The solution (7.28) is free of parameters and is plotted against χ for different values of T in figure 8.1(a).

We obtain $\theta(\chi, T)$ by integration (7.21), using (7.28); it is plotted against χ for different values of T in figure 8.2(a).

An important functional of the solution is the velocity $U(0,t)$ at the outlet which can be obtained from

$$\frac{\partial\theta(0,T)}{\partial\chi} = \int_0^T \frac{\partial\psi}{\partial\chi}(0,T')dT'$$

where

$$\frac{\partial\psi}{\partial\chi}(0,T) = -\delta(T)f(0,T) + H(T)\frac{\partial f}{\partial\chi}(0,T)$$

Hence

$$\frac{\partial\theta}{\partial\chi}(0,T) = -1 + \int_0^T \frac{\partial f}{\partial\chi}(0,T')dT' \tag{7.29}$$

where θ is plotted in figure 8.2. The velocity $u(0,t)$ at the outlet can be expressed in terms of (7.29) by

$$\begin{aligned} u(0,t) &= -\lambda_0\frac{\partial\pi}{\partial x}(0,t) \\ &= \frac{\lambda_0 A}{c}\frac{\partial\theta}{\partial\chi}(0,t/\alpha\tau) \end{aligned} \tag{7.30}$$

7.2 Rate of production

The rate of production of oil is the volume of oil leaving the outlet at $x = 0$ per unit time and is given by

$$\overset{\circ}{Q} = \text{Area } u(0,t)[1-\phi(0,t)] \tag{7.31}$$

where Area is the area of the sandpack and $\phi(0,t)$ is given by (7.13) for $t < t_0$. The cumulative production up to a time $\hat{t} < t_0$ is given by

$$\begin{aligned} Q_{\hat{t}} = \int_0^{\hat{t}} \overset{\circ}{Q}(t)dt = \\ \text{Area}\frac{\lambda_0 A}{c}\int_0^{\hat{t}} \frac{\partial\theta}{\partial\chi}(0,t/\alpha\tau)\left[1 - \frac{A}{\beta\tilde{p}}(t+\tau\alpha)\right]dt \end{aligned} \tag{7.32}$$

For small values of $A/\beta\tilde{p}$, the cumulative production is a linearly increasing function of the drawdown rate A.

8 Diffusion

For small values of the relaxation time τ, the second time derivative in (7.6) becomes less and less important in the solution; the amplitude of the discontinuity in the solution decays to diffusion rapidly and the hyperbolic property of the solution is apparent only at very early times. The change of variables used in section 8 is not appropriate for the limit $\tau \to 0$. When $\tau = 0$, the linearized problem (7.6) reduces to

$$\alpha \frac{\partial \pi}{\partial t} = \beta \tilde{p} \lambda_0 \frac{\partial^2 \pi}{\partial x^2} \tag{8.1}$$

and (7.12) reduces to

$$\pi + \beta \tilde{p} \phi = 0 \tag{8.2}$$

This problem is subject to the initial condition (7.8) and (7.9), the inlet condition (7.10) and the outlet conditions (7.11). A new change of variables

$$\left.\begin{aligned} \pi &= -\alpha A \theta, \\ x &= \sqrt{\beta \tilde{p} \lambda_0}\, \chi, \\ t &= \alpha T \end{aligned}\right. \tag{8.3}$$

leads to the following parameter-free diffusion problem

$$\left.\begin{aligned} &\tfrac{\partial \theta}{\partial T} = \tfrac{\partial^2 \theta}{\partial \chi^2}, \\ &\theta(\chi, 0) = 0, \\ &\tfrac{\partial \theta}{\partial \chi}(L, T) = 0, \\ &\theta(0, T) = \begin{cases} T & (0 < T < T_0) \\ T_0 & (T > T_0) \end{cases} \end{aligned}\right\} \tag{8.4}$$

where

$$l = \frac{L}{\sqrt{\beta \tilde{\rho} \lambda_o}} \quad \text{and} \quad T_o = \frac{t_o}{\alpha}$$

We may form an auxilliary problem for

$$\psi = \frac{\partial \theta}{\partial T} \tag{8.5}$$

analogous to that (7.20)

$$\left.\begin{array}{l} \frac{\partial^2 \psi}{\partial T} = \frac{\partial^2 \psi}{\partial T^2} \\ \psi(\chi, 0) = 0, \end{array}\right\} \tag{8.6}$$

$$\frac{\partial \psi}{\partial \chi}(l, T) = 0, \tag{8.7}$$

$$\psi(0, T) = H(T) - H(T - T_0) \tag{8.8}$$

The solution of the ramp-up problem (8.4) may be obtained from the solution of the auxiliary by integration as in (7.21).

In the limit

$$l \to \infty \quad \text{and} \quad T_0 \to \infty,$$

equation (8.7) and (8.8) may be replaced by

$$\left.\begin{array}{ll} \psi(\infty, T) & = 0 \\ \psi(0, T) & = H(T) \end{array}\right\} \tag{8.9}$$

The solution of (8.6) and (8.9) is unique and is given by

$$\psi = \frac{1}{\sqrt{\pi T}} \int_0^{\chi} \exp\left(\frac{-\chi^2}{4T}\right)\, d\chi = \text{erfc}\left\{\frac{\chi}{2\sqrt{T}}\right\} \tag{8.10}$$

The solution of the corresponding ramp up problem with $\theta(0, T) = T$ is given by integration of (8.10)

$$\theta(\chi, T) = \int_0^T \psi(\chi, T')\, dT', \tag{8.11}$$

Graphs of $\psi(\chi, T)$ and $\theta(\chi, T)$ which can be compared with figures 8.1(a) and 8.2(a) are given in figures 8.1(b) and 8.2(b).

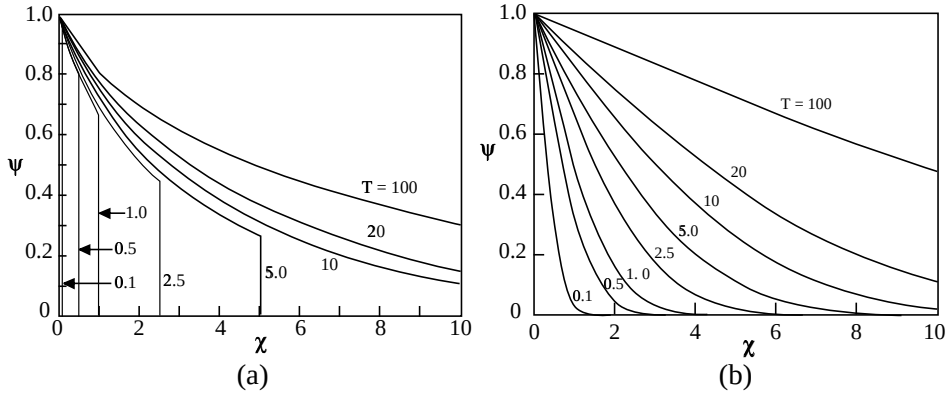

Figure 8.1: Comparison of wave propagation and diffusion for a step change in pressure $\psi(\chi, T)$: $\psi(\chi, T) = 0 \ \forall \ \chi$ when $T < 0$, $\psi(0, T) = H(T)$, $\psi(\infty, T) = 0$. (a) wave propagation: ψ satisfies (7.22) and is given by (7.28). (b) diffusion: ψ satisfies (8.6) and (8.9) and is given by (8.10).

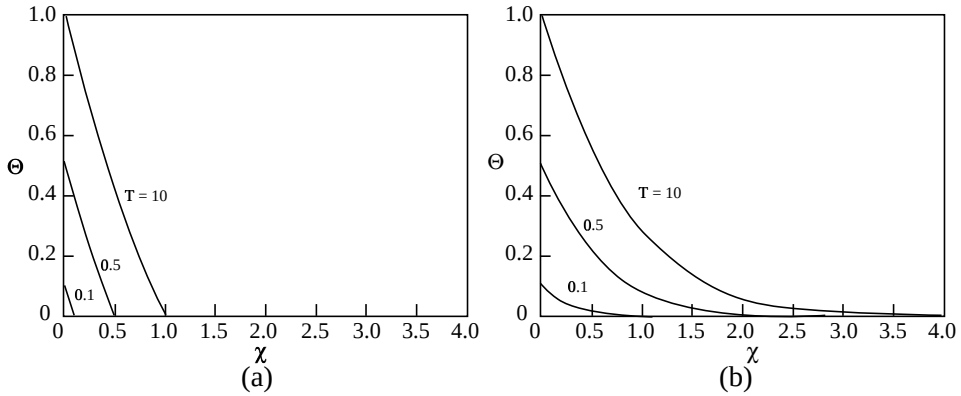

Figure 8.2: Comparison of wave propagation and diffusion for a ramp change in pressure: $\psi(\chi, T) = 0$ for $T < 0$, $\psi(0, T) = T$, $\psi(\infty, T) = 0$. (a) wave propagation: $\psi = \theta$ where θ satisfies (7.15), (7.16), $\theta(\infty, T) = 0$ and (7.26). (b) diffusion: $\psi = 0$ where θ is given by (8.11).

9 Steady flow in a horizontal sandpack

We drive foamy oil from a reservoir at saturation $\tilde{p}$ to another reservoir at the outlet pressure p_L. The dispersed gas fraction at the ends $\phi(0) = \phi_0$ and $\phi(L) = \phi_L$ are unknowns, not continuous at reservoir interfaces. It will be convenient to work with dimensionless variables

$$y = \frac{p}{\tilde{p}},\ \chi = x/L. \tag{9.1}$$

The dimensionless form of equations (7.4) and (7.5) for steady flow are

$$\hat{\tau}\Lambda(\phi)\left(\frac{dy}{d\chi}\right)^2 = \frac{y[1+(\beta-1)\phi]-1+\phi}{1-\phi}, \tag{9.2}$$

$$-\Lambda(\phi)\frac{dy}{d\chi}\frac{d\phi}{d\chi} + (1-\phi)\frac{d}{d\chi}\left\{\Lambda(\phi)\frac{dy}{d\chi}\right\} = 0, \tag{9.3}$$

$$\left.\begin{array}{r}(y,\phi) = (1,\phi_o) \text{ at } \chi = 0\\ (y,\phi) = (y_L,\phi_L) \text{ at } \chi = 1\end{array}\right\} \tag{9.4}$$

where

$$\Lambda(\phi) = \lambda(\phi)/\lambda(\phi_0)$$

and

$$\hat{\tau} = \frac{\tau\tilde{p}\lambda(\phi_0)}{L^2} \tag{9.5}$$

is a dimensionless relaxation time; the underlying sytem of equations is hyperbolic and accomodates discontinuous solutions only when $\tau > 0$.

Equation (9.2) may be written as

$$\frac{d}{d\chi}\left\{\Lambda(\phi)(1-\phi)\frac{dy}{d\chi}\right\} = 0,$$

hence

$$\Lambda(\phi)(1-\phi)\frac{dy}{d\chi} = C = constant. \tag{9.6}$$

Equation (9.6) says that the oil velocity

$$-\lambda \frac{dp}{dx}(1-\phi)$$

in steady flow is a constant independent of x. Combining (9.6) and (9.2) we get

$$\hat{\tau} C \frac{dy}{d\chi} = y[1+(\beta-1)\phi] - 1 + \phi. \tag{9.7}$$

Equations (9.6) and (9.7) together with the conditions (9.4) define the steady flow in a horizontal sandpack.

When the relaxation time τ vanishes, (9.7) reduces to the equilibrium isotherm $f(p,\phi) = 0$ which means that the right hand side of (9.2) vanishes

$$y[1+(\beta-1)\phi] - 1 + \phi = 0 \tag{9.8}$$

Elimination of ϕ between (9.6) and (9.8) leads to a nonlinear first order differential equation in which the integration constant and the constant C are determined by the prescribed conditions (9.4). For the equilibrium case, the condition $y = 1$ at $x = 0$ implies that $\phi_0 = 0$ so that ϕ is continuous into the reservoir at $x = 0$.

In the general case, (9.6) and (9.7) imply that

$$\frac{\hat{\tau} C^2}{\Lambda(\phi)(1-\phi)} = y[1+(\beta-1)\phi] - 1 + \phi \tag{9.9}$$

Evaluating (9.8) first at $\chi = 0$ where $y = 1$, we get

$$\frac{\hat{\tau} C^2}{\Lambda(\phi_0)(1-\phi_0)} = \beta\phi_0 \tag{9.10}$$

and then at $\chi = 1$, we get

$$\frac{\hat{\tau} C^2}{\Lambda_L(1-\phi_L)} = y_L[1+(\beta-1)\phi_L] - 1 + \phi_L \tag{9.11}$$

Equations (9.10) and (9.11) determine C^2 and one relation between ϕ_0 and ϕ_L.

Equation (9.9) may be solved for

$$y = F(\phi) = \left\{ \frac{\hat{\tau} C^2}{\Lambda(\phi)(1-\phi)} + 1 - \phi \right\} / [1 + (\beta - 1)\phi] \tag{9.12}$$

After differentiating (9.12) with respect χ, replacing $dy/d\chi$ with (9.6), we get

$$\frac{C}{\Lambda(\phi)(1-\phi)} = F'(\phi)\frac{d\phi}{d\chi}$$

and

$$C\chi = \int_{\phi_0}^{\phi} \Lambda(\eta)(1-\eta)\, F'(\eta) d\eta. \tag{9.13}$$

A second relation between ϕ_0 and ϕ_L is implied by (9.13) when $\chi = 0$ and $\chi = 1$.

The case $\tilde{\tau} = 0$ is of special interest. In this case the relaxation to equilibrium in which the pressure and dispersed gas fraction lie on a solubility isotherm is immediate. In this case (9.13) may be written as

$$C\chi = -\int_{\phi_0}^{\phi} \beta \frac{\Lambda(\eta)(\eta - 1)}{[1 + (\beta - 1)\eta]^2} d\eta \tag{9.14}$$

where $\phi = \phi_L$ at $\chi = 1$.

To investigate the effects of the relaxation parameter $\hat{\tau}$ on steady flow we treat the case in which the mobility $\lambda(\phi)$ is a constant independent of ϕ; in this case $\Lambda = 1$ and (9.13) reduces

$$C\chi = (1-\phi)F(\phi) + \int_{\phi_0}^{\phi} F(\eta) d\eta + C_0 \tag{9.15}$$

where

$$C\chi = \frac{\hat{\tau} c^2}{\beta} \ln \frac{1 + (\beta - 1)\phi}{1 + (\beta - 1)\phi_0} \frac{1 - \phi_0}{1 - \phi} + \left(\hat{\tau} c^2 + \frac{\beta^2}{(\beta - 1)^2} \right) \times \left(\frac{1}{1 + (\beta - 1)\phi} - \frac{1}{1 + (\beta - 1)\phi_0} \right) + \frac{\beta}{(\beta - 1)^2} \ln \frac{1 + (\beta - 1)\phi}{1 + (\beta - 1)\phi_0} \tag{9.16}$$

where $\phi = \phi_L$ at $\chi = 1$.

10 Comparison with the experiments of Maini & Sarma [1994]

Maini & Sarma [1994] reported results of experiments in a sandpack like that shown in figure 6.1 where pressure at inlet and outlet are controlled. A table of properties of the sandpack is given in Table 10.1. "Prior to the start of the flow experiments, each oil sample was cleaned of its suspended materials. The oil was then recombined with methane gas in the recombination equipment at a pressure of 4.83MPa." They did steady flow experiments using Lloydminster and Lindbergh crude oil in which the inlet pressure was at saturation

$$p = \tilde{p} = 4.83MPa = 4.83 \times 10^7 dynes/cm^2$$

varying the "drawdown" pressure at the outlet.

Table 10.2 gives the properties of the two "live" oils at saturation.

Parameter	Value
Length (m)	2.0
Cross-sectional area (m^2)	16.1×10^{-4}
Sand size (μ m)	74–105
Porosity (fraction)	0.33
Pore volume (mL)	1062
Permeability (μm^2)	3.35
Confining pressure used (MPa)	14.0

Table 10.1: Properties of the Porous Medium.

Oil	Density (g/cc)	Viscosity (Poise)	Core Average ϕ at maximum drawdown	β
Lloydminster	0.968	30.07	0.138	3.40
Lindbergh	0.978	39.70	0.148	3.17

Table 10.2: Properties of "live oil" at saturation.

The pressure distribution along the core sample which was measured in steady flow by Maini and Sarma [1994] is shown in figure 10.1 and 10.2. Six pressure transducers were placed at intervals along the pack. Each transducer measures the

pressure drop between two taps equally spaced along the pack; the pressure drop across two taps is called a ”differential pressure.” The plots given in figures 10.1 and 10.2 are of straight line segments between pressure taps.

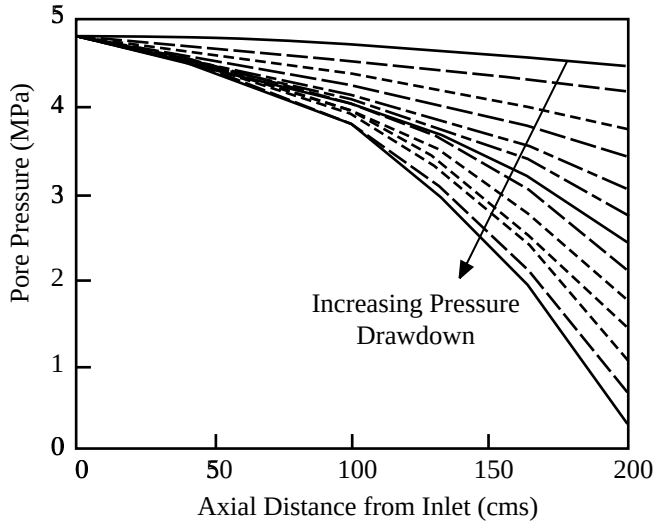

Figure 10.1: (Maini & Sarma, 1994). Pressure distributions in steady flows of Lindbergh oils at various pressure drawdowns.

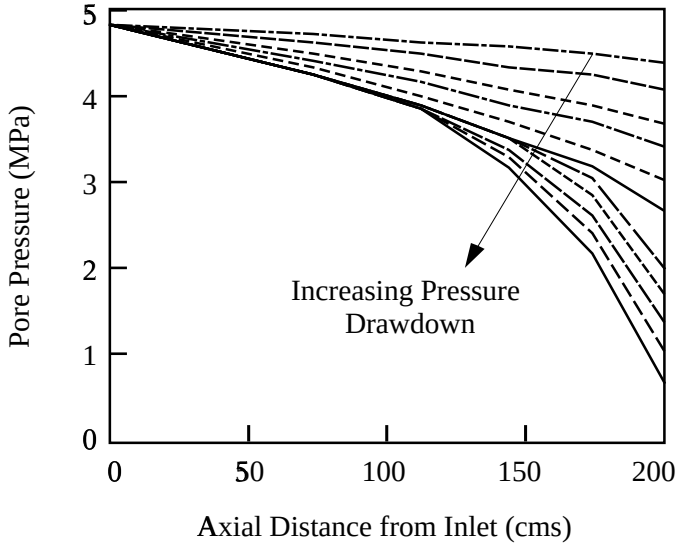

Figure 10.2: (Maini & Sarma, 1994). Pressure distributions in steady flow of Lloydminster oils at various pressure drawdowns.

Comparison of theory with the experiments of Maini and Sarma [1994] requires that we input a mobility function $\lambda(\phi) = k/\mu(\phi)$ which was not given by them. We are going to take $k = 3.35$ to be the constant value given in Table 10.1 and we will express

$$\mu(\phi) = \mu_0 m(\phi) \tag{10.1}$$

where μ_0 is the viscosity of live oil at saturation (given in Table 10.2) when $\phi = 0$ and of course $m(0) = 1$. The viscosity of the dispersion should grow with ϕ and, even more, the viscosity of oil istelf should increase when dissolved gas is released to the dispersion. However the viscosity of foamy oils in porous media is an unsettled subject and even the sign in the change of viscosity is controversial (see Sheng, *et al.* [1999a]).

We are going to use the celebrated empirical formula of Thomas [1965]

$$m(\phi) = 1 + 2.5\phi + 10.05\phi^2 + 0.00273\mathbf{e}^{16.6\phi} \tag{10.2}$$

for the viscosity of a dispersion of solid spheres of uniform size. This formula gives good results for small and moderate values of ϕ, say $\phi < 0.5$, which is not too close from a statistically well-packed array. Various empirical formulas for dispersions of solid spheres have been proposed and are compared in the paper of Poletto and Joseph [1994]. It can be said that none of these formulas is accurate near the well-packed condition which in fact develops a rheology more complicated than can be described by an "effective" viscosity.

The viscosity of well dispersed spherical bubbles might be described by the viscosity of a similar dispersion of solid spheres. In any case the expression 10.1 and 10.2 cannot be expected to hold for values of $\phi > 0.68$, and they may not hold for values of $\phi > 0.4$. It is of interest to evaluate if good agreement between theory and experiment can be achieved by choosing an appropriate viscosity function.

We are first going to compare theoretical pressure distributions of the equilibrium theory with $\tau = 0$ with the measured distribution as given in figure (10.1) and (10.2). The conparison will be given for drawdown in three cases, from 4.83MPa to (1) 0.75 MPa, (2) 1 MPa and (3) 3 MPa. Our attention is directed to Lloydminster and Lindbergh oils for which the solubility isotherms are given in figure 2.5.

To evaluate the response to a pressure drawdown it is useful to look at the maximum gas fraction in the sandpack. This will occur at the outlet where the pressure is lowest and $\phi(L) = \phi_L$. From figure 2.5 we find the values given in table 10.3.

	p_L(MPa)	$\phi_L(\beta = 3.4)$	$\phi_L(\beta = 3.4)$
(1)	0.75	0.615	0.632
(2)	1	0.53	0.547
(3)	3	0.152	0.161

Table 10.3: The outlet gas fraction with drawdown pressures.

From these values we may conclude that foamy and free gas will certainly occur at the outlet in case (1) and possibly in case (2). Case (3) should be well in the region of validity for non-foaming bubbly mixtures and the Thomas equation (10.2) should work if the assumptions that dispersed bubbles act like dispersed solid spheres when they are not closely packed; the Thomas equation might work for (2) but it will not work for (1) (see figure 10.8).

It is perhaps helpful to note that the last exponential terms of (10.2) accounts for less than 10% of $m(\phi)$ when $\phi < 0.268$.

The exponential term in the Thomas formula should not be used when ϕ indicates close packing. The viscosity of close packed solid spheres could tend to infinity but dispersed bubbles would foam or form free gas when close packed and the increase in the effective viscosity would be more moderate than for solid spheres. The value of ϕ for which a more moderate than exponential increase would be expected is not known but we might anticipate a value near $\phi = 0.5$. In fact we find excellent agreement with the observed distributions of pressure when we use the full Thomas formula (10.2) in drawdowns to 1MPa and 3MPa and a truncated version of Thomas' formula with the exponential neglected

$$\mu = \mu_0(1 + 2.5\phi + 10.05\phi^2) \tag{10.3}$$

for drawdown to $\phi_L = 0.75$ MPa. These comparisons are exhibited in figures 10.3, 10.4, 10.5 and 10.6. Figure 10.3 is our theoretical result for Lloydminster oil which can compare with the experimental result given in figure 10.2.

A more detailed comparison of theory and experiment is shown in figures 10.4, 10.5 and 10.6. The observed pressure is slightly higher for Lloydminster than Lindbergh in the cases $p_L = 1$MPa and $p_L = 0.75$MPa but is smaller for $p_L = 3$MPa. In all cases the assumption that the mobility λ is constant underpredicts the pressure. Good agreements between theory and experiments is achieved with oil fitting under the assumption that mobility varies with ϕ as $\lambda = k/\mu(\phi)$ with k given in table 10.1, μ_0 given in table 10.2 and $\mu(\phi)$ given by the Thomas expression (10.2) and (10.3).

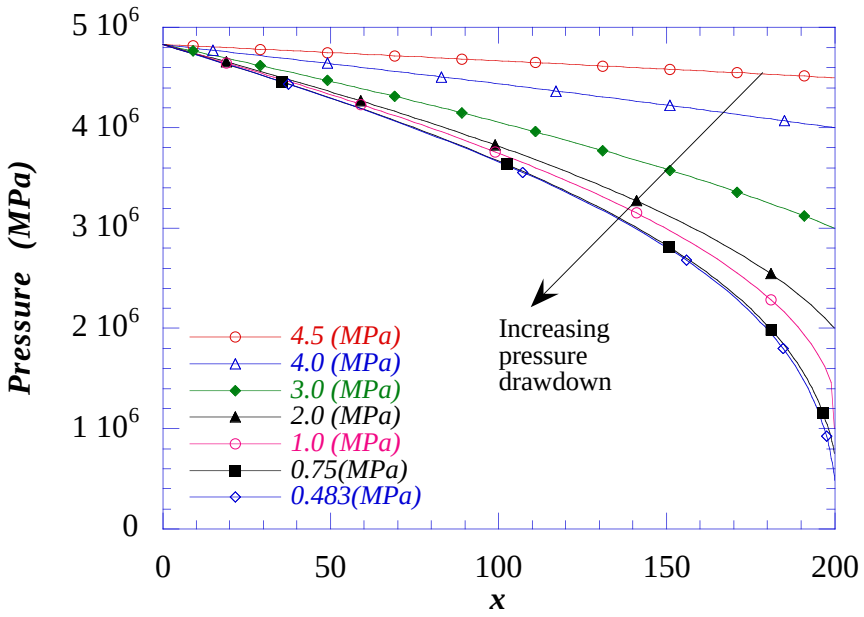

Figure 10.3: Theoretical pressure distributions in steady flows of oil (with $\beta = 3.4$ and variable $\mu(\phi)$ as in (10.2)) at pressure drawdowns to values greater than 0.75 and the truncated formula (10.3) from 0.75 to 0.483 MPa. This figure can be compared with the experimental result shown in figure 10.2.

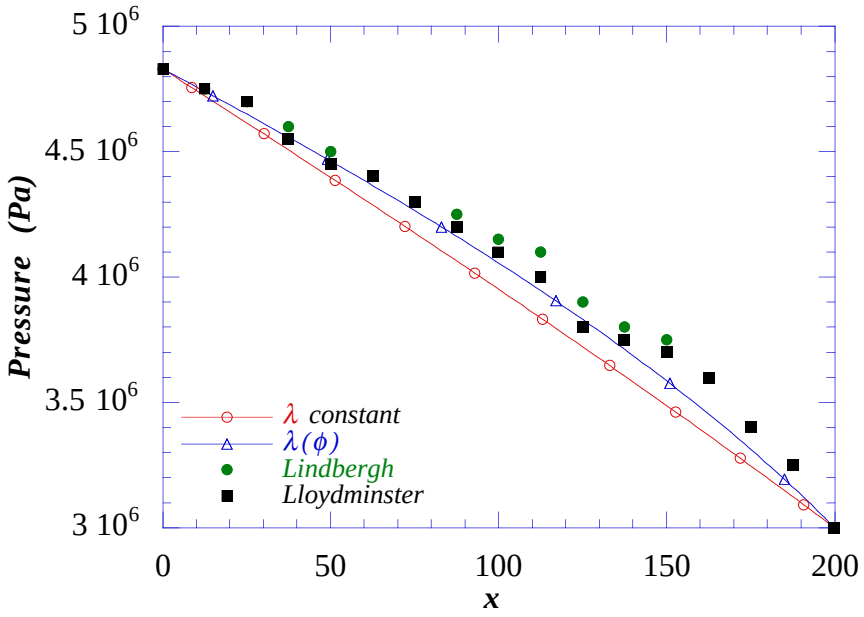

Figure 10.4: Comparisons of the theoretical and experimental pressure distributions at drawdown pressure p_L =3MPa. $\beta = 3.4$ is used in the theory for both constant and variable oil viscosity μ.

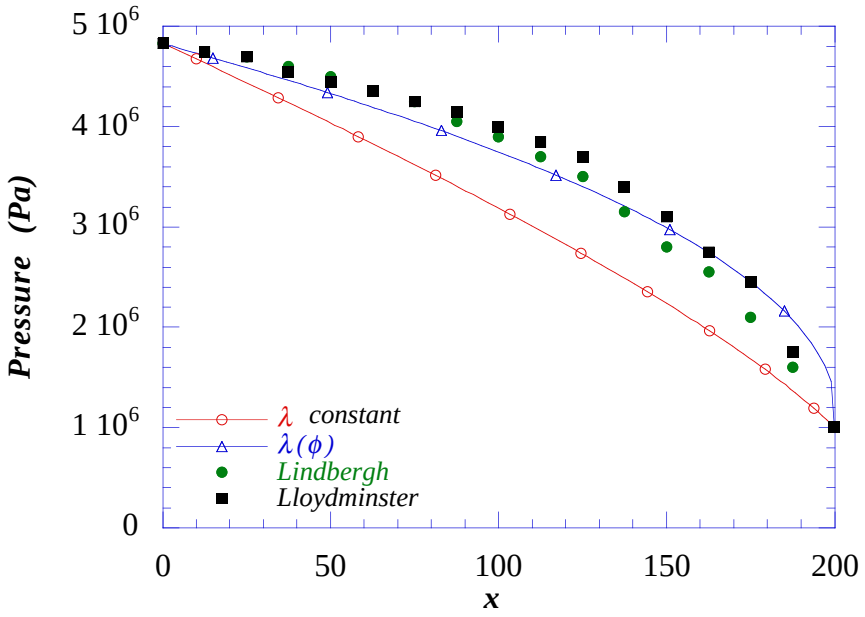

Figure 10.5: Comparisons of the theoretical and experimental pressure distributions at drawdown pressure $p_L = 1$MPa. $\beta = 3.4$ is used in the theory for both constant and variable oil viscosity μ.

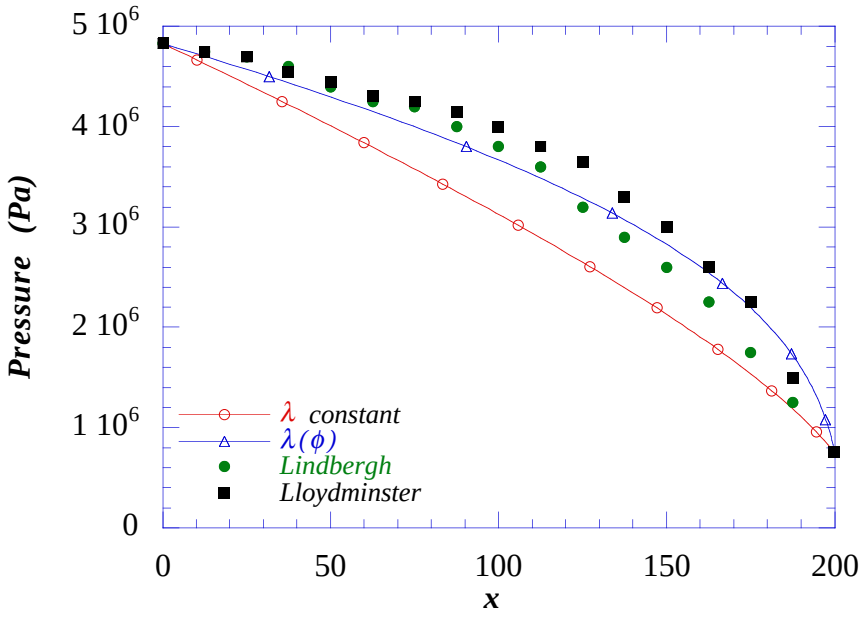

Figure 10.6: Comparisons of the theoretical and experimental pressure distributions at drawdown pressure $p_L = 0.75$MPa. $\beta = 3.4$ is used in the theory for both constant and variable oil viscosity μ.

In figure 10.7 we compared the theoretical prediction for the pressure when $\beta = 3.17$ (Lindbergh) and $\beta = 3.4$ (Lloydminster); the differences are very small with slightly higher value of p when $\beta = 3.17$.

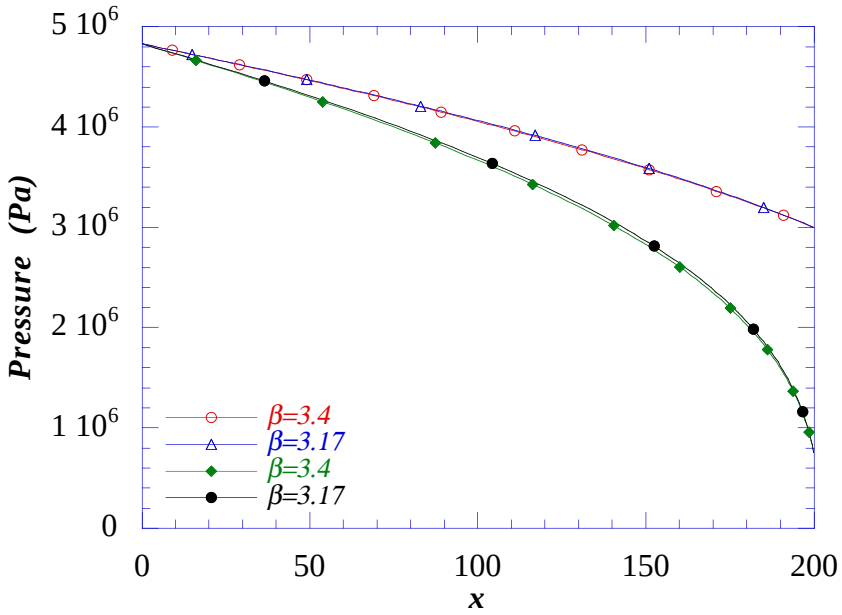

Figure 10.7: Comparisons of theoretical pressure distributions with Lloydminster ($\beta = 3.17$) and Lindbergh ($\beta = 3.4$) oils at drawdown pressure $p_L = 0.75$ MPa and 3 MPa. For the same drawdown pressure, the pressure difference is not significant with different β.

Figure 10.8 compares theoretical and experimental values (Maini & Sarma [1994] figure 2) for the oil production rate (10.4) as a function of the pressure drawdown. The volume flow rate is given by

$$\mathring{Q} = \text{Area } [-\lambda(\phi)\, dp/dx\, (1-\phi)] \tag{10.4}$$

where the area is $16.1 \times 10^{-4} m^2$ (table 10.1) and the quantity in the brachials is the constant oil velocity (see (9.6)). The mass flow rate is obtained by multiplying (10.4) by the oil density $\rho_o = 0.968$ g/cc and converting to experimental units. The production rate is over predicted when $\lambda = \lambda_o$ is constant. The exponential term in the Thomas expression under predicts when the oil foams. The agreement between

theory and experiment with variable $\lambda(\phi)$ using expression (10.1) and (10.2) and no fitting parameters is excellent.

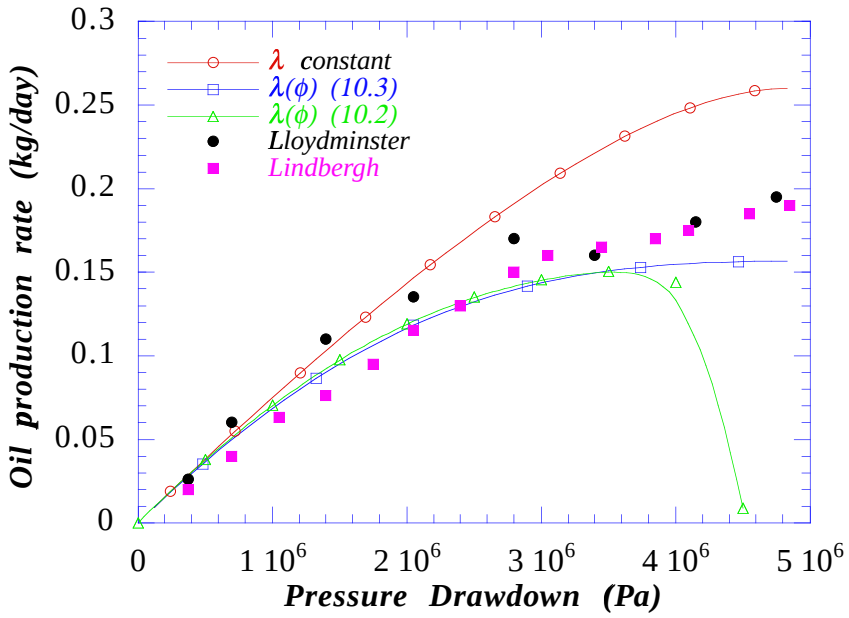

Figure 10.8: Comparisons of oil production rates in steady flows at various pressure drawdowns.

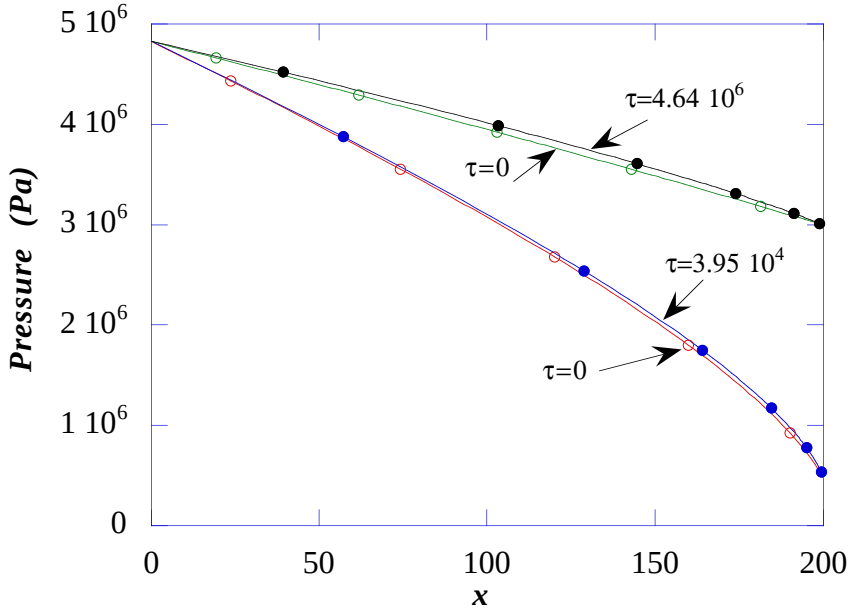

Figure 10.9: Comparisons of theoretical pressure distributions with different relaxation time τ at $\beta = 3.4$ and constant oil viscosity. The maximum relaxation time that can be reached is $\tau = 4.64 \times 10^6$ when drawdown pressure $p_L = 3$MPa and $\tau = 3.95 \times 10^4$ when drawdown pressure $p_L = 0.75$MPa. There is no significant pressure difference for the different τ.

In figure 10.9 we show the results of our investigation of the influence that has the relaxation times τ. Our hope to back out τ from the steady flow experiments was not realized. The solution ceases to exist when $\phi = 1$, as it should and the difference in the pressure distribution in the region in which a relaxation solution exists is smaller than the errors in the experiments.

We turn next to the blow down experiment of Maini and Sarma [1994] (their figure 9, our figure 10.10). They describe their experiment as follows (the emphasis indicated is ours).

> A different type of experiment was needed to estimate the total recovery potential of solution gas drive. This experiment started with the sand pack at maximum "live oil" saturation. The pack was allowed to blow down to atmospheric pressure through the outlet end, and the inlet end remained closed. Figure 9 shows the recovery and pressure-drop behavior. *More than 20% of the original oil was recovered in this primary depletion experiment.* The value is surprisingly high for the viscous oil system and suggests that the critical gas saturation was much higher than what would be measured by an external gas drive experiment. Typically, the external drive experiments in such systems show the critical gas saturation to be less than 5%. Therefore, this experiment also suggests that a mechanism is present in heavy-oil systems to increase the critical gas saturation. *We suggest that this mechanism is the formation of an oil-continuous foam.*

We have already remarked that the solubility isotherm with $\beta = 3.4$ or 3.17 leads to dispersed gas fractions of the order 0.93; foaming is inevitable.

10.1 Blowdown experiment

The blowdown experiment is unsteady. The experiments shown in figure 10.10 show that the pack is still producing oil after 200 hours; the terminal steady and uniform state has not been achieved.

The results of the experiments at early times are not accurate enough to test our theory of hyperbolic propagation. Morever, the blowdown leads to foam and connected gas, a regime to which our theory should not apply.

We have the idea that after hours, wave propagation has decayed to diffusion, and that as a preliminary to a complete study of the nonlinear transient problem we could examine the idea that some information could be obtained from the diffusion theory given in section 8 modified to take into account the presence of a fixed wall. We solved the following problem

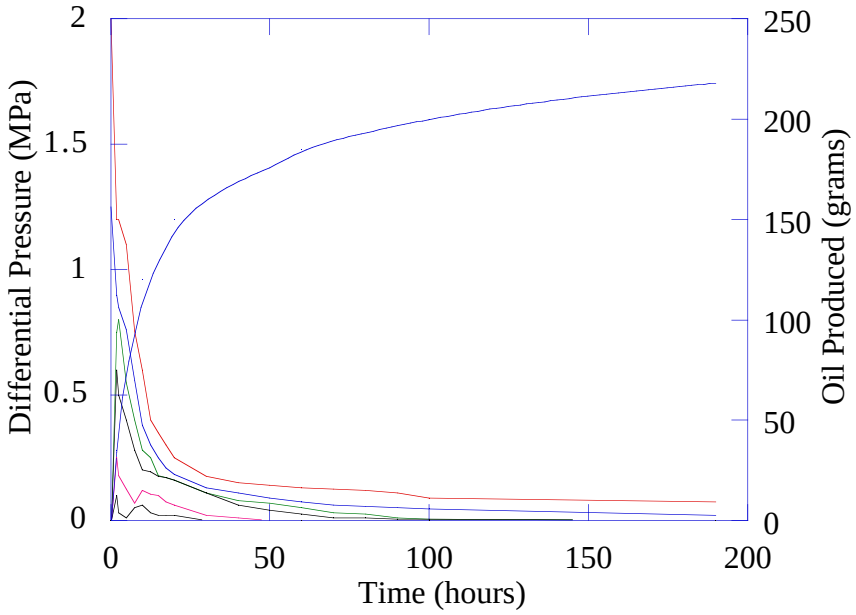

Figure 10.10: (Maini & Sarma, 1994). Change in the pressure drop across different core segments and cumulative oil production with time during the blowdown experiment with the Lloydminster system.

$$\left.\begin{aligned} \frac{\partial p}{\partial t} &= \frac{\beta\tilde{p}\lambda_o}{\alpha}\frac{\partial^2 p}{\partial x^2}, \\ p(x,0) &= \tilde{p}, \\ p(0,t) &= p_L\left[1-H(t)\right], \\ \frac{\partial p}{\partial x}(L,t) &= 0 \end{aligned}\right\} \tag{10.5}$$

where $\beta = 3.4, \tilde{p} = 4.83$MPa, $\lambda_o = k/\mu_o, k = 3.35 \times 10^{-8} cm^2$, $\mu_o = 30$ poise, $\alpha = 1/3$, $\beta\tilde{p}\lambda_o/\alpha = 11/20 = 0.55$ and $p_L = 0.1$MPa. The problem (10.5) was resolved numberically and the results were displayed in figure 10.11. The differential pressure distributions predicted by the diffusion theory follow the qualitative trends observed in the experiments. The oil produced is given

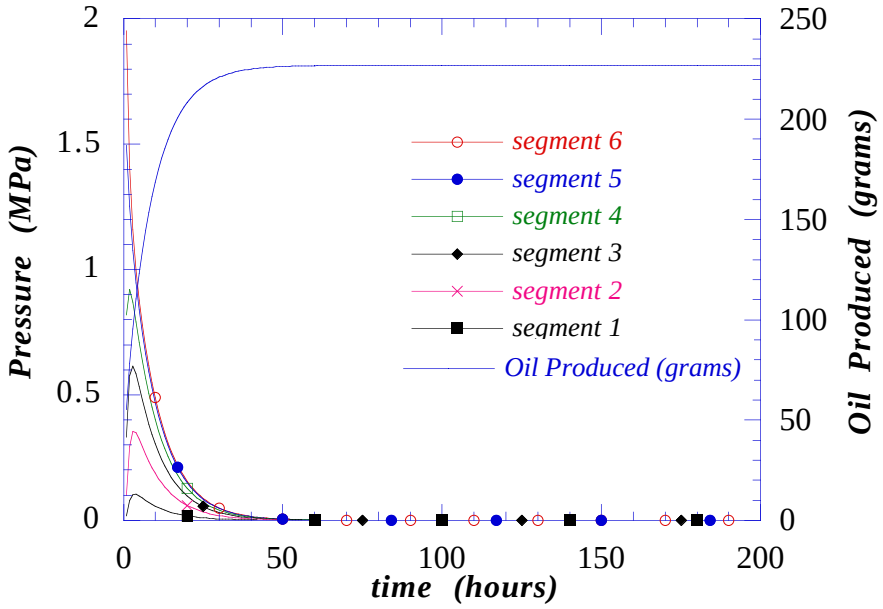

Figure 10.11: Change in the pressure drop across different core segments and cumulative oil production with time during the blowdown with the linearized Lloydminster system.

$$\rho_o \, Q(t) = \rho_o \int_o^t \mathring{Q}(t) \, dt \tag{10.6}$$

where

$$\mathring{Q} = \text{-Area } \lambda(1-\phi) \, dp/dx \tag{10.7}$$

is evaluated at $x = 0$, the open end of the sandpack. The theory overpredicts the cumulative productin because blowdown produces large amounts of connected gas which is not allowed in the theory.

11 Conclusion and discussion

The theory which we have developed could be called a continuum mixture theory for foamy oils flow with dispersed gas of low mobility relative to the liquid which

leads to three coupled nonlinear partial differential equations for $\mathbf{u}, p$ and the gas fraction ϕ, five scalar equations in five unknowns.

The model proposed here does not require information about nucleation, bubble growth, liquid compressibility or forces which produce relative velocity. We put up a one-phase or mixture theory in which the dispersed gas is described by a gas fraction field in a single fluid in which the viscosity, density and mobility in D'Arcy's law all depend on the gas fraction. This fluid satisfies the usual D'Arcy law, and the continuity equation together with a kinetic (constitutive) equation required by the condensation and outgassing of methane (or other gases) in heavy crude. The theory depends only on parameters which can be measured in a PVT cell and sandpack. The virtue of the model is simplicity, but it can work only for relatively immobile dispersed gas bubbles in which divergence-free velocities are excluded (see the discussion following (4.4)). Certainly such a theory could not be expected to give rise to a percolation threshold or even to a critical gas fraction. We have shown that it can describe many features of solution gas drive of foamy oils in the regimes when the bubbles in the mixture are dispersed and even when they are trapped in foam.

The equations of our theory are highly nonlinear and the underlying system is hyperbolic giving rise to propagating bubble fronts, and experiments to check the predicted wave speeds have as yet to be carried out. When the wave speeds are known, we may calculate a relaxation time which is a material parameter of our theory.

We solved linearized versions of our equations for the pressure drawdown in a sandpack with one end closed and were able to resolve the nonlinear flow for steady flow in an open sandpack by quadrature. The solutions of the steady flow problem depend only weakly on the relaxation time which when put to zero gives rise to our equilibrium solution. The results of the equilibrium theory are in excellent agreement with the experiments of Maini & Sarma [1994] when the mobility is chosen for a constant permeability and a viscosity given by Thomas' [1965] celebrated expression for the viscosity of a dispersion of solid spheres.

The theory given here is in the spirit of applied mathematical modeling and though it depends strongly on empirical data through and only through our solubility constant β, it is without fitting parameters.

More work can and should be done with this theory, but the results given here go far toward establishing that a simple theory, based on the dispersed gas fraction, avoiding complicated modeling of nucleation, bubble growth, transition to free gas and complicated transfer functions, can capture many of the essential features of foamy oil flow.

12 Appendix

In this appendix we carry out an analysis of equations (4.10) for type; we show that under the usual conditions the system is hyperbolic with x, t plane tesselated by nonintersecting characteristic lines.

Putting the gravity related term to zero (4.10) can be written as

$$\tau\alpha\frac{\partial p}{\partial t} - \lambda\tau\left(\frac{\partial p}{\partial x}\right)^2 - \tilde{p} + p + \frac{\beta p\phi}{1-\phi} = 0 \tag{12.1}$$

$$\alpha\frac{\partial \phi}{\partial t} - \lambda\frac{\partial p}{\partial x}\frac{\partial \phi}{\partial x} + (1-\phi)\lambda'\frac{\partial \phi}{\partial x}\frac{\partial p}{\partial x} + \lambda(1-\phi)\frac{\partial^2 p}{\partial x^2} = 0 \tag{12.2}$$

where $\lambda' = d\lambda/d\phi$. To analyze this system we use the method of simple jumps. To put the system into canonical form we need to form a quasilinear system in which the highest derivatives are linear and (12.1) is not quasilinear. We can get a quasilinear system by differentiating (12.1) with respect to x, writing

$$p' \stackrel{\text{def}}{=} \frac{\partial p}{\partial x}$$

Then

$$\tau\alpha\frac{\partial p'}{\partial t} - 2\lambda\tau p'\frac{\partial p'}{\partial x} + \frac{\beta p}{(1-\phi)^2}\frac{\partial \phi}{\partial x} - \lambda'\tau(p')^2\frac{\partial \phi}{\partial x} + p' + \frac{\beta p'\phi}{1-\phi} = 0 \tag{12.3}$$

$$\lambda(1-\phi)\frac{\partial p'}{\partial x} + \alpha\frac{\partial \phi}{\partial t} + \left[\lambda'(1-\phi)p' - \lambda p'\right]\frac{\partial \phi}{\partial x} = 0 \tag{12.4}$$

Now we look for solutions which allow for simple jumps of the derivatives of p, p' and ϕ assuming that p, p' and ϕ are continuous. These (characteristic) lines are designated as

$$\psi(x,t) = \text{const} \tag{12.5}$$

and we seek the explicit form of the function ψ.

Now define a notation for a simple jump across the line $\psi(x,t) = \text{const}$

$$[\![\circ]\!] = (\circ)_1 - (\circ)_2$$

The jump equations corresponding to (12.3) and (12.4) are

$$\tau\alpha \left[\!\left[\frac{\partial p'}{\partial t}\right]\!\right] - 2\lambda\tau p' \left[\!\left[\frac{\partial p'}{\partial x}\right]\!\right] + \left(\frac{\beta p}{(1-\phi)^2} - \lambda'\tau(p')^2\right) \left[\!\left[\frac{\partial \phi}{\partial x}\right]\!\right] = 0 \quad (12.6)$$

$$\lambda(1-\phi) \left[\!\left[\frac{\partial p'}{\partial x}\right]\!\right] + \alpha \left[\!\left[\frac{\partial \phi}{\partial t}\right]\!\right] + \left(\lambda'(1-\phi)p' - \lambda p'\right) \frac{\partial \phi}{\partial x} = 0 \quad (12.7)$$

The derivatives are discontinuous across but not along characteristic lines. Hence

$$(\tau\alpha\psi_t - 2\lambda\tau p'\psi_x)[\![p'_\psi]\!] + \left(\frac{\beta\phi}{(1-\phi)^2} - \lambda'\tau(p')^2\right)\psi_x[\![\phi_\psi]\!] = 0 \quad (12.8)$$

$$\lambda(1-\phi)\psi_x[\![p'_\psi]\!] + \left\{\alpha\psi_t + \left(\lambda'(1-\phi)p' - \lambda p'\right)\psi_x\right\}[\![\phi_\psi]\!] = 0 \quad (12.9)$$

Equations (12.8) and (12.9) may be solved for the jumps if and only if

$$\left(\alpha\psi_t + \left\{\lambda'(1-\phi)p' - \lambda p'\right\}\psi_x\right)\left(\tau\alpha\psi_t - 2\lambda\tau p'\psi_x\right) - \lambda(1-\phi)\psi_x^2\left\{\frac{\beta\phi}{(1-\phi)^2} - \lambda'\tau(p')^2\right\} = 0 \quad (12.10)$$

On the line $\psi = \text{const}$

$$d\psi = \psi_x\, dx + \psi_t\, dt = 0$$

Hence

$$-\psi_t/\psi_x = \frac{dx}{dt} \equiv \overset{\circ}{x} \quad (12.11)$$

After inserting (12.11) into (12.10) and some algebraic rearrangements, we find that

$$\alpha\overset{\circ}{x} + \frac{p'}{2}\left[3\lambda - \lambda'(1-\phi)\right] = \pm\left\{\frac{\lambda\beta\phi}{\tau(1-\phi)} + \left(\lambda^2 + (\lambda')^2(1-\phi)^2\right)\frac{(p')^2}{4} - \frac{1}{2}\lambda\lambda'(1-\phi)(p')^2\right\}^{1/2} \quad (12.12)$$

If the quantity under the square root is positive, there are two roots for $\overset{\circ}{x}$ which define the characteristics. If the mobility is independent of ϕ

$$\lambda' = 0$$

then there are always two roots and the original system is strictly hyperbolic.

The analysis just given does mean that discontinuities in p and ϕ are not allowed as we saw already in the linearized analysis leading to the telegraph equation. The underlying system is not quasilinear and the existence of shock waves in the solution set is an open question.

$$\left(-\alpha \overset{\circ}{x} + \lambda'(1-\phi)p' - \lambda p'\right)\left(-\tau\alpha \overset{\circ}{x} - 2\lambda\tau p'\right) - \lambda(1-\phi)\left\{\frac{\beta\phi}{(1-\phi)^2} - \lambda'\tau {p'}^2\right\} = 0 \qquad (12.13)$$

$$\alpha^2 \overset{\circ}{x}^2 + \overset{\circ}{x}\left[2\alpha\lambda p' - \alpha\lambda'(1-\phi)p' + \alpha\lambda p'\right] - 2\lambda p'\left[\lambda'(1-\phi)p' - \lambda p'\right] - \frac{\lambda\beta\phi}{\tau(1-\phi)} + \lambda\lambda'(1-\phi){p'}^2 = 0 \qquad (12.14)$$

$$\alpha^2 \overset{\circ}{x}^2 + \alpha p' \overset{\circ}{x}\left[3\lambda - \lambda'(1-\phi)\right] - \lambda\lambda' {p'}^2 (1-\phi) + 2\lambda^2 {p'}^2 - \frac{\lambda\beta\phi}{\tau(1-\phi)} = 0 \qquad (12.15)$$

$$\left\{\alpha \overset{\circ}{x} + \frac{p'}{2}\left[3\lambda - \lambda'(1-\phi)\right]\right\}^2 - \frac{{p'}^2}{4}\left[3\lambda - \lambda'(1-\phi)\right]^2 - \lambda\lambda' {p'}^2 (1-\phi) + 2\lambda^2 {p'}^2 - \frac{\lambda\beta\phi}{\tau(1-\phi)} = 0 \qquad (12.16)$$

$$\left\{\alpha \overset{\circ}{x} + \frac{p'}{2}\left[3\lambda - \lambda'(1-\phi)\right]\right\}^2 - \frac{\lambda^2 {p'}^2}{4} - \frac{{p'}^2 {\lambda'}^2}{4} (1-\phi)^2 + \frac{1}{2}\lambda\lambda'(1-\phi){p'}^2 \frac{\lambda\beta\phi}{\tau(1-\phi)} = 0 \qquad (12.17)$$

Acknowledgement. The work of D.D. Joseph was supported in part by the DOE (Engineering Research Program of the Department of Basic Energy Sciences), the NSF under Grant Opportunities for Academic Liasons with Industry and the Minnesota Supercomputer Institute. We wish to thank Prof. G.I. Barenblatt for bringing Leibenson [1941] to our attention and for helpful discussion.

References

1. Carlslaw and Jaeger 1969 *Operational Methods in Applied Mathematics*, Oxford University Press (2nd ed).

2. Claridge, E.L. and Prats, M. June 19-21, 1995 "A Proposed Model and Mechanism for Anomalous Foamy Heavy Oil Behavior," paper SPE 29243 presented at the International Heavy Oil Symposium, Calgary, AB *Proc.*, 9-20; also the unsolicited manuscript of SPE (USMS) 29243, 1994.

3. Firoozabadi, A., Ottesen, B., & Mikkelsen, M. December 1992 "Measurement of Supersaturation and Critical Gas Saturation", SPE Formation Evaluation, 337–344.

4. Huerta, M., Otero, C., Rico, A., Jiménez, I., De Mirabal, M. & Rojas, G. October 6-9, 1996 "Understanding Foamy Oil Mechanisms for Heavy Oil Reservoirs during Primary Production", paper SPE 36749, presented at the 1996 SPE Annual Technical Conference and Exhibition, Denver, Colorado, 671–685.

5. Joseph, D.D. 1990 Fluid dynamics of viscoelastic liquids, Springer-Verlag. *Appl. Math Sciences*, **84**.

6. Kataoka, T., Kitano, T., Sasahara, M., & Nishijima, K. 1978 "Viscosity of particle filled polymer melts," *Rheol. Acta* **17**, 149– 155.

7. Kraus, W.P., McCaffrey, W.J., & Boyd, G.W. 1993 "Pseudo-Bubble Point Model for Foamy Oils," paper CIM 93-94 presented at the 44th Annual Technical Conference of the Petroleum Society of CIM, Calgary, AB, May 9-12.

8. Lebel, J.P. March 2, 1994 "Performance implications of various reservoir access geometrics", Paper presented at the 11^{th} *Annual Heavy Oil & Oil Sands Tech. Symp.*.

9. Leibenson, L.S., 1941 The motion of gas-saturated fluid in a porous media. Bulletin, USSR Acad. Science, ser. giography & geophysics, No. 3.

10. Maini, B.B., June 1996 "Foamy Oil Flow in Heavy Oil Production," *JCPT* 35, No. 6, 21-24.

11. Maini B.B. & Sarma, H. 1994 "Role of Nonpolar Foams in Production of Heavy Oils," in: "Advances in Chemistry Series" **242**: 405–420.

12. Metzner, A.B. 1985 "Rheology of suspensinos in polymeric liquids," *J. Rheol.* **29**, 739–735.

13. de Mirabal, M., Gordillo, R., Fuenmayor, M., Rojas, G., Rodriguez H. & Sanchez, R. April 23–26, 1996 “Integrated Study for the Characterization and Development of the MFB-53 Reservoir, North Hamaca-Orinoco Belt, Venezuela”, paper SPE 36095, presented at the Fourth Latin American & Caribbean Petroleum Engineering Conference, Port-of-Spain, Trinidad & Tobago.

14. Peng, D.Y., Fu, C.T., Bird, G.W. & Hsi, C. August, 4-9, 1991 “Effect of Gas components on thermodynamic properties of Alberta Heavy Crudes and Bitumens,” in: 5th Unitar Heavy Crude & Tar Sands International Conference, Caracas, Venezuela, Proc. 1: 47-55.

15. Poletto M. & Joseph, D.D. March/April 1995 Effective density and viscosity of a suspension, it J. Rheol. **39(2)**, 323-343.

16. Pooladi-Darvish M. & Firoozabadi, A. June 11, 1997 “Solution gas drive in heavy oil reservoirs”, paper no. 97-113, presented at the 48th Annual Technical meeting of the Petroleum Society of CIM in Calgary, Canada.

17. Sheng, J.J., Hayes, R.E., Maini A.B. & Tortike, W.S. 1996 A dynamic model to simulate foamy oil flow in porous media, SPE 36750.

18. Sheng, J.J., Maini, B.B., Hayes R.E. & Tortike, W.S. May 1999a ”Critical Review of foamy Oil Flow”, *Transport in Porous Media,* **35,2**, 157-187.

19. Sheng, J.J., Hayes, R.E., Maini, B.B. & Tortike, W.S. May 1999b ”Modeling Foamy Oil Flow in Porous Media”, *Transport in Porous Media,* **35,2**, 227-258.

20. Svrcek, W.Y. & Mehrotra, A.K. 1982 Gas solubility, viscosity and density measurements for Athabasca bitumen, *J. Canadian Petroleum Technology*, **21**,(4) 31–38.